Holocene environmental history of Washington Land, NW Greenland: a study based on lake sediments

Kajsa Frisendahl

Dissertations in Geology at Lund University,
Master's thesis, no 661
(45 hp/ECTS credits)

Department of Geology
Lund University
2023

Holocene environmental history of Washington Land, NW Greenland: a study based on lake sediments

Master's thesis

Kajsa Frisendahl

Department of Geology
Lund University
2023

Contents

1 Introduction **7**
1.1 Background 8
1.1.1 Last glacial maximum 8
1.1.2 Deglaciation 9
1.1.3 Holocene thermal maximum 9
1.2 Study site 9
2 Methods **11**
2.1 Core collection, correlation, and subsampling 11
2.2 Macrofossil analysis 11
2.3 Dating and construction of age-depth model 11
2.4 Elemental analysis 12
2.5 X-ray fluorescence analysis 12
2.6 Pollen analysis 12
3 Results **12**
3.1 Chronology 12
3.2 Sediment description and macrofossils 14
3.3 Elemental geochemistry 15
3.4 Pollen 16
4 Discussion **19**
4.1 Deglaciation 19
4.2 Vegetational history 19
4.3 Environmental history 20
4.4 Late Holocene 22
4.5 Potential implications for palaeogenetic studies 24
5 Conclusions **24**
6 Acknowledgements **24**
7 References **25**
Appendix A **31**
Appendix B **32**

Holocene environmental history of Washington Land, NW Greenland: a study based on lake sediments

Kajsa Frisendahl

Frisendahl, K., 2023: Holocene environmental history of Washington Land, NW Greenland: a study based on lake sediments. *Dissertations in Geology at Lund University*, No. 661, 32 pp. 45 hp (45 ECTS credits).

Abstract: Washington Land is a peninsula in north-western Greenland, separated from Ellesmere Island by the narrow Nares Strait, which makes it an ideal location to study the colonization of Greenland by plants, mammals, and humans following the last deglaciation. A sediment sequence was retrieved from a small lake during the Ryder19 expedition in 2019, primarily to provide an archive for palaeogenetic analyses. The aim of this thesis is to determine the age of the deglaciation and to clarify the subsequent environmental history of the area against which palaeogenetic data can be compared. An age-depth model was created based on ^{14}C, ^{210}Pb and ^{137}Cs data, which reveals that the site was deglaciated around 7300 cal BP. The sediment sequence was divided into two major lithostratigraphic units. The basal Unit 1, which represents the initial nearly two millennia following the deglaciation, consists of clay with a total organic carbon content of around 1%. Elemental geochemistry data based on X-ray fluorescence analysis indicate increased catchment erosion and low aquatic productivity. Pollen analysis reveals that *Salix* (willows), Cyperaceae (sedges) and Poaceae (grasses) were established shortly after the deglaciation, but *Salix* dominated until about 6500 cal BP. The relative abundance of *Salix* and the low aquatic productivity indicate that the lake was relatively close to the receding ice margin. The overlying Unit 2 consists of gyttja with a total organic carbon content exceeding 10%. The transition from clay to gyttja took place around 5500 cal BP and was likely caused by the retreat of the ice margin from the vicinity of the lake. Elemental geochemistry data and maximum organic matter content of the sediments indicate relatively high aquatic productivity and elevated chemical weathering of catchment soils between 5500 and 3500 cal BP. This interpretation is consistent with higher temperatures and increased precipitation during the Holocene Thermal Maximum inferred from other studies in the region. Sediment organic matter content and weathering decrease towards the top of the sequence, which suggests colder and drier conditions after about 3500 cal BP. The pollen record shows no significant changes after the initial decline in *Salix*, and pollen influx remained largely unaltered, which indicates relatively stable vegetation conditions during the last 5-6 millennia.

Keywords: northern Greenland, Washington Land, lake sediments, paleoecology, XRF core scanning, geochemistry

Supervisors: Dan Hammarlund, Anne Birgitte Nielsen, Karl Ljung

Subject: Quaternary Geology

Kajsa Frisendahl, Department of Geology, Lund University, Sölvegatan 12, SE-223 62 Lund, Sweden. E-mail: kajsafrisendahl@outlook.com

Holocen miljöhistoria på Washington Land, NV Grönland: en studie baserad på sjösediment

Kajsa Frisendahl

Frisendahl, K., 2023: Holocen miljöhistoria på Washington Land, NV Grönland: en studie baserad på sjösediment. *Examensarbeten i geologi vid Lunds universitet*, Nr. 661, 32 sid. 45 hp.

Sammanfattning: Washington Land är en halvö på nordvästra Grönland, endast skild från Ellesmereön av det smala Nares Sund. Detta gör det till en utmärkt plats för undersökningar av hur växter, djur och människor koloniserade Grönland efter den senaste istidens slut. En sedimentsekvens för paleogenetiska studier provtogs från en liten sjö under Ryder19-expeditionen 2019. Målen med denna uppsats är att utröna när den grönländska inlandsisen drog sig tillbaka från området kring sjön och att undersöka hur miljön har utvecklats sedan dess, mot vilket paleogenetiska data ska jämföras. En åldersmodell för sedimenten framtogs baserat på datering med kol-14, bly-210 och cesium-137, och den avslöjar att sjön deglacierades senast 7300 år före nutid. Sedimentsekvensen kan delas in i två litostratigrafiska enheter. Enhet 1 representerar de två första årtusendena och består av lera med en organisk kolhalt omkring 1%. Geokemiska data baserade på röntgenfluorescensanalys indikerar kraftig fluvial erosion, grumligt vatten och låg akvatisk produktivitet. Pollenanalys avslöjar att *Salix* (vide), Cyperaceae (halvgräs) och Poaceae (gräs) var etablerade i området kort efter att inlandsisen lämnade platsen, men *Salix* dominerade fram till ca 6500 år före nutid. Mängden *Salix* och den låga produktiviteten indikerar att sjön var relativt nära iskanten. Enhet 2 består av gyttja vars organiska kolhalt överstiger 10%. Övergången från lera till gyttja är daterad till omkring 5500 år före nutid, och den orsakades sannolikt av att inlandsisens kant drog sig längre tillbaka. Geokemiska data i kombination med ökad organisk kolhalt mellan 3500 och 5500 år före nutid tyder på ökad akvatisk produktivitet och kemisk vittring i avrinningsområdet. Detta stämmer väl överens med tidigare studier, vilka pekar på förhöjda temperaturer och ökad nederbörd under den holocena värmeperioden. Minskande trender i organisk kolhalt och kemisk vittring mot toppen av sedimentsekvensen tyder på kallare och torrare klimat efter ca 3500 år före nutid. Pollenackumulationen visar inte på några större förändringar efter den initiala minskningen av *Salix*-pollen, vilket tyder på relativt stabila förhållanden under de senaste 6000 åren.

Nyckelord: Norra Grönland, Washington Land, sjösediment, paleoekologi, röntgenfluorescensanalys, geokemi

Handledare: Dan Hammarlund, Anne Birgitte Nielsen, Karl Ljung

Ämnesinriktning: Kvartärgeologi

Kajsa Frisendahl, Geologiska institutionen, Lunds Universitet, Sölvegatan 12, 223 62 Lund, Sverige. E-post: kajsafrisendahl@outlook.com

1 Introduction

Washington Land is an ice-free peninsula in northern Greenland, bordered eastward by the Petermann Fjord and westward by the Humboldt Glacier. The area is separated from the Canadian Arctic only by the relatively narrow Nares Strait, and this makes Washington Land an ideal location for studying the colonization of Greenland by mammals and humans during the Holocene, as the seasonally ice-covered strait is the only way to access Greenland for all non-flying fauna (Bennike, 2002). However, the timing of the deglaciation and the subsequent environmental development is poorly constrained.

In 2019 several sediment sequences were retrieved from small lakes in north-western Greenland during the Ryder19 expedition, organised by the Swedish Polar Research Secretariat. This material will form the basis for a palaeogenetics and ancient DNA project building on collaboration between the Department of Geology in Lund and the Centre for Palaeogenetics (CPG) in Stockholm. This study will be based on the sediment sequence from Red-Throated Loon Lake (unofficial name), Washington Land (Fig. 1).

The aims of my project are to establish a well-constrained chronology based on radiocarbon and radioisotope dating and to provide a framework of

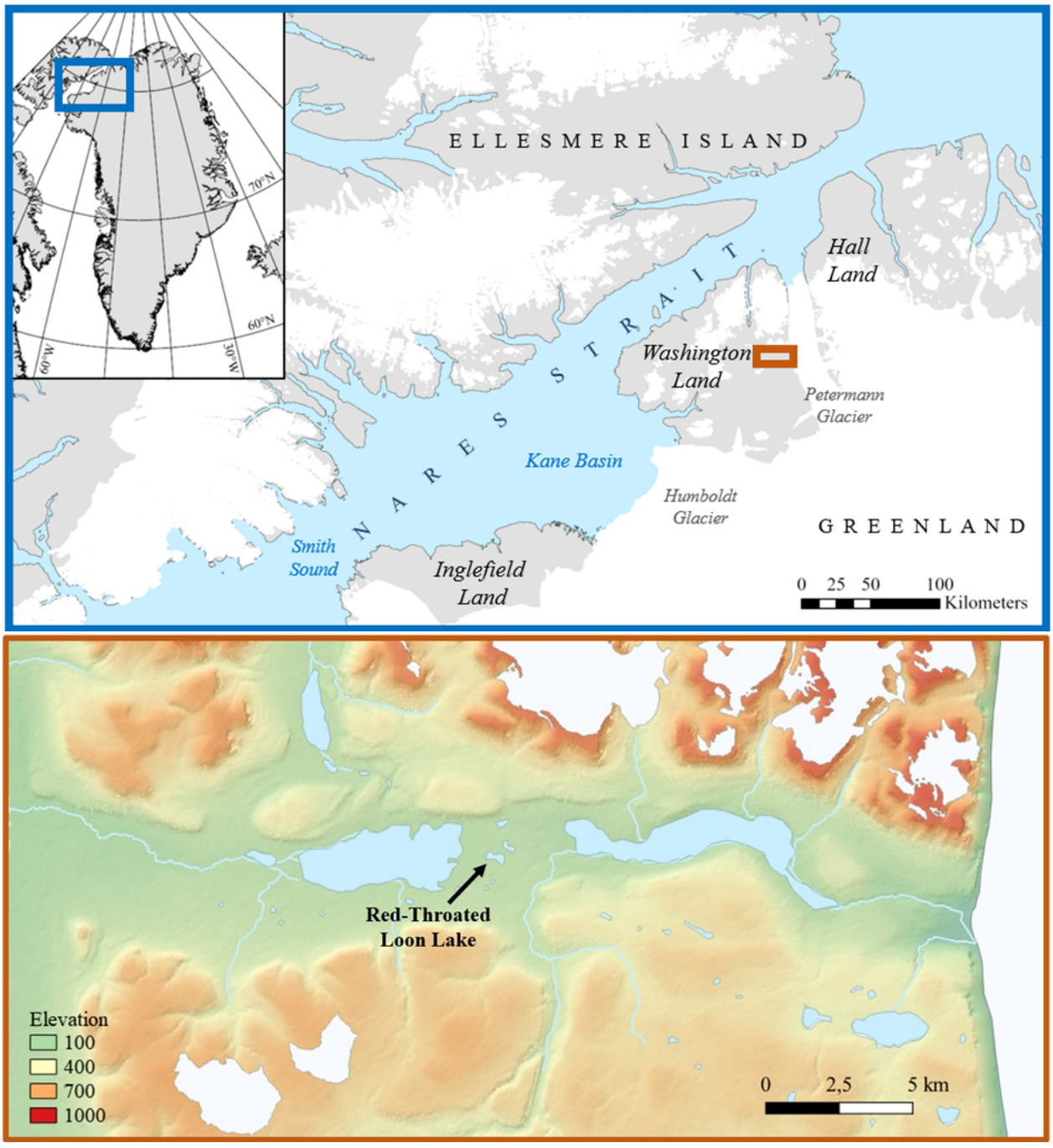

Fig. 1. Map of the Nares Strait region showing the position of the study area in Greenland and the location of the study site in Washington Land. Basemap: ESRI©. Glacier data: RGI Consortium© Elevation data: NSIDC©.

proxy records representing the environmental history of the site and region, to which the palaeogenetic data can be compared. This could provide valuable insight to how mammal and human colonisations were related to changes in the region´s vegetation and climate. Furthermore, I aim to assess the inferred deglaciation age and the subsequent environmental history in the light of established deglaciation models and previously published palaeoecological data, as few studies have managed to provide multi-proxy records from lakes this far north. Such insight would also increase our understanding of the possible consequences of future changes in climate. Washington Land also represents a gap on the map, and significantly more studies have been carried out on the neighbouring Hall Land and Inglefield Land (Bennike, 2000).

Additionally, northern Greenland is vulnerable to climate change. Marine terminating glaciers, such as the Petermann outlet glacier, drain vast areas (Hill et al., 2017), and their retreat is currently accelerating (Rignot & Kanagaratnam, 2006). Northern Greenland is contributing to sea level rise more than previously estimated, and has the possibility to contribute even more in the future due to the large volumes of ice that would respond to an increase in temperature, especially considering arctic amplification (Mouginot et al., 2019). Furthermore, the Nares Strait is an important transport path of water masses in the arctic (Komuro & Hasumi, 2005; McGeehan & Maslowski, 2012). Shrubs are spreading and migrating progressively further north, which will likely affect the otherwise vegetation-poor northern Greenland to a much greater extent than the south (Klein et al., 2008). Earlier spring and deepening of the active layer contribute to changes in species composition (Hobbie et al., 2017; Høye et al., 2007). Warming has to some extent also led to enhanced lake productivity and organic deposition, affecting lake ecology and nutrient cycling (Hobbs et al., 2010).

1.1 Background

1.1.1 Last glacial maximum

According to Lecavalier et al. (2014) the Greenland Ice Sheet (GrIS) reached its maximum Weichselian ice volume around 16,500 cal BP. Glacial lineations and recessional moraines confirm that the GrIS covered at least half of the shelf in the northeast, most likely even more (Evans et al., 2009; Winkelmann et al., 2010). Off the western coast of Greenland the ice sheet most likely reached the shelf edge (Dowdeswell et al., 2014). Funder and Hansen (1996) propose that glaciers on the northern coast were confined to valleys due to limited snow accumulation. The ice sheets of both Greenland and Iceland likely blocked the North Atlantic cyclones from reaching the very northern parts of Greenland, causing cold but dry conditions. Larsen (2010), however, claims that there was shelf-based ice even in northern Greenland, but that it started to degrade already by 16,000 cal BP.

Erratic boulders from Greenland have been found 15 km inland on Ellesmere Island at elevations of up to 800 m (England & Bradley, 1978), which proves that the GrIS extended over the Nares Strait to Ellesmere Island and coalesced with the Innuitian Ice Sheet (Fig. 2). The Kane Basin, south of the Nares Strait, was supposedly occupied by an ice saddle, from where the ice sheet flowed both north and southwards. Strong postglacial isostatic uplift of the Nares strait region confirms the former presence of very thick ice (England, 1999). Prior to the deglaciation, the Petermann outlet glacier likely extended into the Nares Strait and according to glacial lineations on the sea floor probably had a northeast-directed flow (Jakobsson et al., 2018). After the breakup of the Innuitian Ice Sheet and the GrIS the surface elevation of the GrIS was significantly lowered as a result of the thinning ice sheet (Vinther et al., 2009).

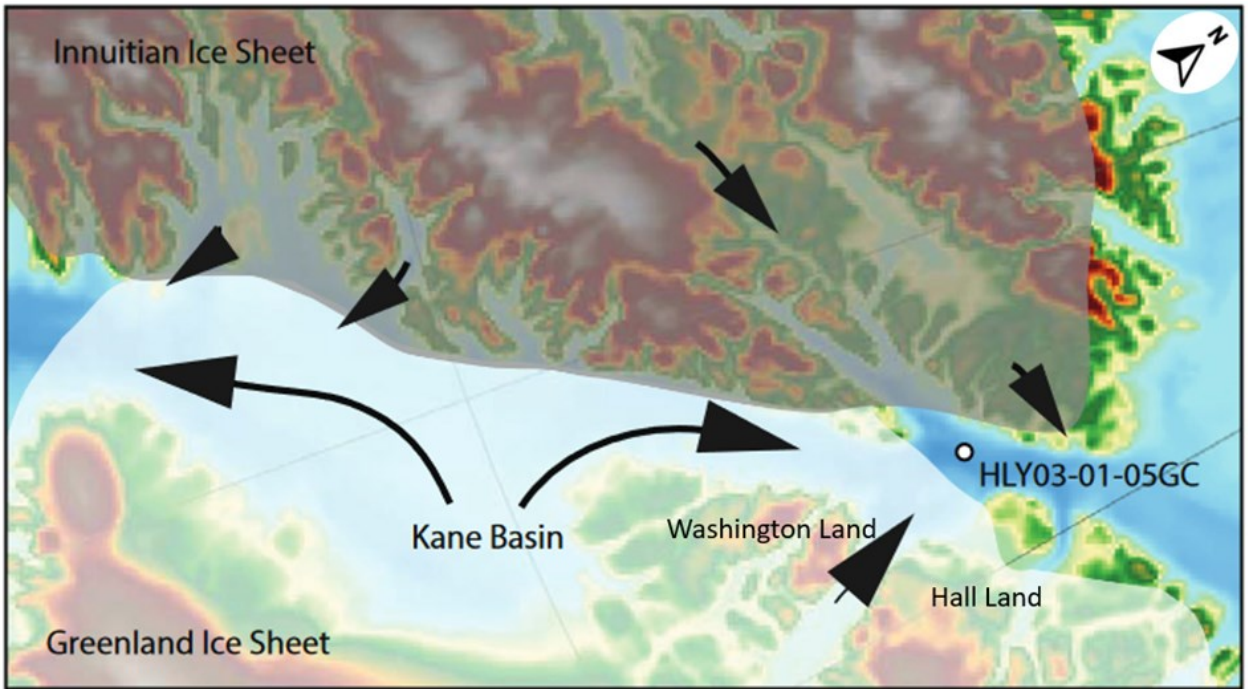

Fig. 2. The GrIS and the Innuitian Ice Sheet coalesced in Nares Strait. From Jennings et al. (2011).

1.1.2 Deglaciation

Dowdeswell et al. (2014) propose that deglaciation in western Greenland had begun already by 14,800 cal BP. Cofaigh et al. (2013) conclude that even though the retreat of adjacent ice tongues might be asynchronous, those of western Greenland started to retreat at around 14,000 cal BP. In general, the ice retreat was earlier from the shelf of eastern Greenland than from the shelf of western Greenland. Rapid warming prevailed from 12,000 cal BP leading to the shelf in northern Greenland being ice-free by 10,100 cal BP at the latest (Jennings et al., 2019; Larsen et al., 2010), and by around 10,000 cal BP the GrIS was entirely landbased (Simpson et al., 2009).

The exact timing of the opening of Nares Strait and Smith Sound has been debated. Lecavalier et al. (2014) propose that the Nares Strait was open at 10,000 cal BP while some claim a later opening (Georgiadis et al., 2018; Jennings et al., 2019). According to Jennings et al. (2019) the GrIS had retreated from Baffin Bay into the Smith Sound by approximately 11,500 cal BP. The part of the GrIS that had coalesced with the Innuitian Ice Sheet had retreated by 10,000 cal BP, and the ice front was positioned at the present coastline by a thousand or so years later (Zreda et al., 1999). Both Jennings (2019) and Georgiadis (2018) claim the Nares Strait was completely open by 8300 cal BP. By approximately that time parts of northern Greenland were inundated by a marine transgression, dated to between 10,500 and 10,000 cal BP (Larsen et al., 2010; Möller et al., 2010; Olsen et al., 2012).

An ice rafted debris event is recorded at 9000 cal BP and the ice retreat of the Nares Strait likely ended just before 7000 cal BP (Jennings et al., 2019). The Petermann Ice Tongue, occupying the Petermann Fjord east of Washington Land (Fig. 1) suffered break up just after 6900 cal BP and during an extended period in the mid-Holocene the ice tongue was completely absent (Reilly et al., 2019).

The uplift since the glaciation varies greatly between different regions in northern Greenland and is mainly localized to several domes separated by areas of less uplift. One dome is centred around Hall land (adjacent to Washington land; Fig. 1) where the marine limit is at an altitude of 130 m (Funder & Hansen, 1996). Bennike (2002) states that Washington Land has probably been uplifted by 100 to 150 m since the deglaciation.

1.1.3 Holocene thermal maximum

The start and end of the Holocene Thermal Maximum (HTM) was asynchronous over the Arctic, and its onset is dated to around 9000 cal BP in the Canadian archipelago and Greenland, whereas it was delayed until about 7000 cal BP in central Canada due to the cooling effect of the remaining Laurentide ice sheet (Kaufman et al., 2004). Briner et al. (2006) suggest that the HTM of Baffin Island ended as early as 8500 cal BP followed by slow cooling until present day.
Funder (2011) puts the start of the Holocene thermal maximum to 8500 cal BP for the north of Greenland. Summer temperatures of north-western Greenland during the HTM were considerably higher than today. McFarlin et al. (2018) have by studying chironomid assemblages estimated the temperature difference to be up to 7°C. Dating of driftwood indicates that presently ice-covered fjords in northern Greenland were seasonally ice-free between 6500 cal BP and 2500 cal BP (Landvik et al., 2001). Kelly & Bennike (1992) have found *Carex* peat dated to 5000 cal BP at Wulf land, slightly east of Washington Land, indicating that peatlands had been established in northern Greenland by that time. At around 4000 cal BP the GrIS reached its minimum extent, and the ice front was positioned up to 80 km behind its current position (Simpson et al., 2009).

1.2 Study site

Red-Throated Loon Lake (80.5926 –61.9870) (Fig. 3) measures 400 x 350 m and is at the site of coring 7.41 m deep. The lake is situated in a valley perpendicular to the Petermann fjord. The size of the catchment of the lake does not exceed the size of the lake itself by more than a few tens of meters. The surrounding areas are relatively barren and devoid of much vegetation except for grasses and some scattered creeping *Salix arctica*. The vegetation of Washington Land is generally sparse compared to other parts of Greenland (Bennike, 2002). During a previous expedition F. Dalerum et al. (unpublished data) recorded, in addition to *Salix*, several members of the families Brassicaceae, Caryophyllaceae and Rosaceae, as well as Cyperaceae and Poaceae.

The landscape of Washington Land is a dissected plateau with broad U-shaped valleys (Bennike, 2002). A low-lying silt plain with frost polygons is situated north of the lake. The bedrock of the northern part of Washington Land, also called Petermann Peninsula, is mainly composed of limestone, sometimes dolomitic and sometimes accompanied by breccia or calcarenite (Hurst, 1980). The limestone was mainly deposited during the late Ordovician and early Silurian. No bedrock outcrops were observed in the vicinity of Red-Throated Loon Lake, and the ground is covered by tills, mainly composed of calcareous clasts. In the north-western parts of Washington Land some shale and sandstone can be found. The bedrock is in that area mainly covered by till and glaciofluvial sediments. Permafrost features such as pingos and polygons are common in Washington Land, as well as glacial striations, moraines and melt water channels (Bennike, 2002).

The closest weather station is in Hall Land, approximately 100 km to the north-east. Between 1991 and 1996 the mean air temperature was -35.9°C in January, 5.1°C in July, and the annual mean temperature was 18.7°C. The snow-free season generally lasts from July to September. The area is characterized by relatively low precipitation and strong winds which cause uneven distribution of snow during wintertime (Jensen & Cappelen, 2021). The closest weather station to record precipitation is in Qaanaaq, almost 400 km south-west of Washington Land. The yearly precipitation varied between 41.7 and 205.5 mm during the years 1964-1975 (Blake et al., 1992).

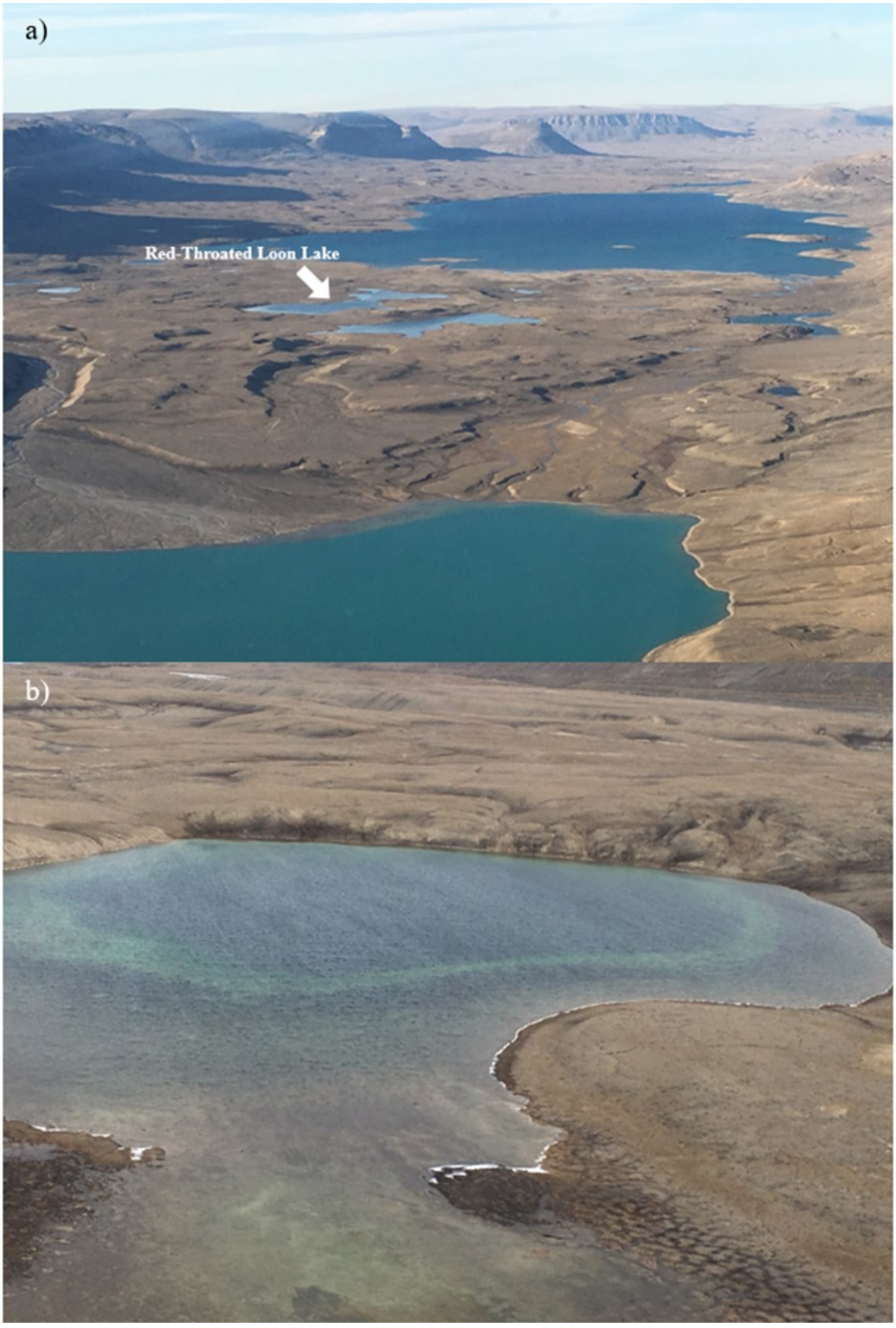

Fig. 3. Photographs of Red-Throated Loon Lake a) The valley in which Red-Throated Loon Lake is situated, the camera is facing south-west, b) the deeper, western embayment of Red-Throated Loon Lake, which measures ~250 m across.
Photo: D. Hammarlund.

2 Methods

2.1 Core collection, correlation, and subsampling

Eight overlapping sediment cores were obtained using an inflatable boat and a Russian corer (Fig. 4). No undisturbed surface sediment were retrieved with the Russian corer. The cores were wrapped in plastic and brought to the Department of Geology and stored for about 3 years at 4°C. The cores were opened, and their surfaces were cleaned by scraping off approximately 1-3 mm of sediment using a plastic spatula. The cores were mutually correlated based on lithostratigraphic changes, and a reference sequence was established using two cores spanning the entire combined length of the sediment sequence, measuring 173. The reference cores were described, photographed, and used for sampling for elemental analysis and pollen, as well as for X-ray fluorescence (XRF) scanning.

To obtain undisturbed surface sediments a gravity core, measuring 42 cm, was retrieved from Red-throated Loon Lake. The core was divided into 1 cm slices and packed into plastic bags in the field. The samples were later transferred to plastic boxes and freeze dried.

Samples for carbon and nitrogen elemental analysis were taken contiguously in slices of 1 cm in the uppermost 29 cm of the reference sequence, and of 2 cm for the rest of the sequence. Samples were also taken every cm from the gravity core. Samples for pollen analysis were taken every second cm in the uppermost 128 cm of the reference sequence and every third cm below that. Cubes of approximately 1 cm^3 were cut out of the sediments, and to ensure that the cubes were accurately measured their volumes were estimated by water displacement in tubes filled with 2 cm^3 of distilled water.

2.2 Macrofossil analysis

The reference sequence was divided into sections of two cm in the uppermost 128 cm and 3 cm below that. These divisions were transferred to the rest of the cores, based on lithostratigraphic characteristics, which were sectioned accordingly. All sections of corresponding depths were placed in plastic bags. Thus, the cores that constitute the reference sequence remained intact, except for holes from sampling for elemental analysis and pollen analysis. The amalgamated sediment sections were wet sieved using a 250 µm sieve, and the material not passing through the sieve was placed in plastic boxes with distilled water and a drop of 10% NaOH to prevent calcareous remains from dissolving. The overall characteristics of the material was described, such as sand content, amount of plant macrofossils and presence of ostracods. Some plant remains, such as leaves, were identified if possible.

2.3 Dating and construction of age-depth model

Macroscopic plant remains were collected for radiocarbon dating from ten different depths with sufficient amounts of material (~2 mg dry weight) and put into glass containers. Since plants taking their carbon from lake water might yield too old ages due to the reservoir effect caused by, for example, ancient dissolved carbonates (Philippsen, 2013), macrofossils of potentially aquatic plants such as moss were excluded (Wagner et al., 2000). The samples were processed at the Radiocarbon Dating Laboratory at the Department of Geology, Lund University. The material was pretreated with HCl, and the dated sample sizes were in the range of 0.4 to 2 mg C.

The freeze-dried samples from the gravity core were analysed at the Environmental Radiometric Facility at University College, London. ^{210}Pb and ^{137}Cs were measured using an ORTEC HPGe GWL series well-type coaxial low background intrinsic germanium detector. Lead-210 is a natural radionuclide produced in the atmosphere and 137-Cesium is released from nuclear weapons and nuclear reactor accidents.

A smooth spline age-depth model was produced using Clam 2.2 (Blaauw, 2010) in the statistical software R version 3.6.3 (R Core Team, 2011). The smoothing factor was changed from 0,3 (default) to 0,7 in order to increase the smoothness of the curve. The calibration curve IntCal20.14C was used to obtain calibrated dates (Blaauw, 2010; Reimer et al., 2020). The individual radiocarbon ages were also calibrated using OxCal (Bronk Ramsey, 2009) and the calibration curve IntCal20.14C (Reimer et al., 2020).

Fig. 4. The eight cores obtained with a Russian corer, which overlap according to how they are placed in the picture.

2.4 Elemental analysis

Approximately 5 mg of dry material from every sample was put into a silver capsule and the sample weights were recorded with a microbalance. Only objects cleaned with 95% ethanol were allowed to touch the samples or the capsules. The capsules were placed on a tray on a hot plate set to 50°C and were treated with 2 M HCl acid. To avoid losing any material the acid was initially added in rounds of 10 µl followed by approximately 20, 30, 40 and 50 µl, until the total amount of added acid was at least 300 µl (Brodie et al., 2011). The silver capsules were closed and encased in tin capsules. The samples were analysed using an ECS 4010 – CHNS-O Elemental combustion system elemental analyser, and the measurements were calibrated against a set of standards.

2.5 X-ray fluorescence analysis

The reference cores were brought to the Department of Geology at Stockholm University and scanned using an ITRAX core scanner from Cox Analytical Systems (Gothenburg, Sweden). XRF scans were made using a molybdenum tube set at 30 kV and 25 mA with a dwell time of 30 s. The upper, more homogenous part of the sediment sequence was scanned with a step size of 5 mm, and the lower part with a step size of 2.5 mm.

The XRF results are given as counts per second (cps) and the intensities can be used to estimate the downcore variations in element abundance but need to be processed further in order to remove effects of varying physical properties of the sediments. The intensities of two elements cannot be compared since they are not a direct measure of concentration. To analyse the downcore variation in two elements relative each other log-ratios were calculated. To accurately analyse the downcore variation of single elements, the data were transformed using centered log-ratios (CLR) (Weltje et al., 2015). First the geometric mean (g(z)) of n elements of depth z was calculated (Equation 1), and then the centered log-ratio (CLR A(z)) of element A at depth z (Equation 2).

Only elements that were both relevant to the study and well counted (preferably more than 300 counts per second) were selected for the centered log-ratio calculations. The transformed XRF-data were plotted against age and smoothed using a 5-point running mean. To find any correlations between elements, correlation matrices for the whole sequence and for units were produced using the Data Analysis toolpack add-in in Excel.

2.6 Pollen analysis

28 pollen samples were selected to be prepared for analysis. Primarily samples in the bottom and in the very top of the sequence were chosen, at intervals of at the most every eighth cm. The samples were processed using the standard methods described in Berglund & Ralska-Jasiewiczowa (1986). One Lycopodium spore tablet was added to each sample as an exotic spike. A tablet contains 18,407 spores with a standard deviation of 623 spores. A total of five slides per sample were produced and observed under a microscope. All pollen, as well as some common spore types and the added Lycopodium spores, were counted. All pollen grains were also photographed. When possible, the pollen grains were identified to genus level, e.g., *Salix*, *Saxifraga* etc., and otherwise to family level, as in the case of Cyperaceae, Poaceae etc. The pollen was mainly identified using *Textbook of Pollen Analysis* by Faegri & Iversen (1989) as well as *An atlas of airborne pollen grains and common fungus spores of Canada* by Bassett (1978). The number of unidentified spores per 100 lycopodium were counted in every sample.

Pollen and spore concentrations were calculated using the added Lycopodium spores (Stockmarr, 1971). The pollen and spore influx rates were calculated based on the methods described by Hicks & Hyvärinen (1999), and the results were plotted against age.

3 Results

3.1 Chronology

The ^{137}Cs activity decreases rapidly with depth in the gravity core, and the top of the peak may not be fully recorded, likely because of loss of the uppermost few cm of the sediment sequence during sampling in the field, which precluded proper age determination based on ^{210}Pb (Fig. 5). However, the total ^{210}Pb activity declines in the uppermost part and reaches supported ^{210}Pb activity at around a depth of 7 cm, in general agreement with the decrease in ^{137}Cs.

$$g(z) = \sqrt[n]{counts_{element\ A\ (z)} \cdot counts_{element\ B\ (z)} \cdot \dots\ counts_{element\ n\ (z)}} \qquad \textit{Equation 1}$$

$$CLR\ A\ (z) = \ln\left[\frac{counts\ element\ A\ (z)}{g(z)}\right] \qquad \textit{Equation 2}$$

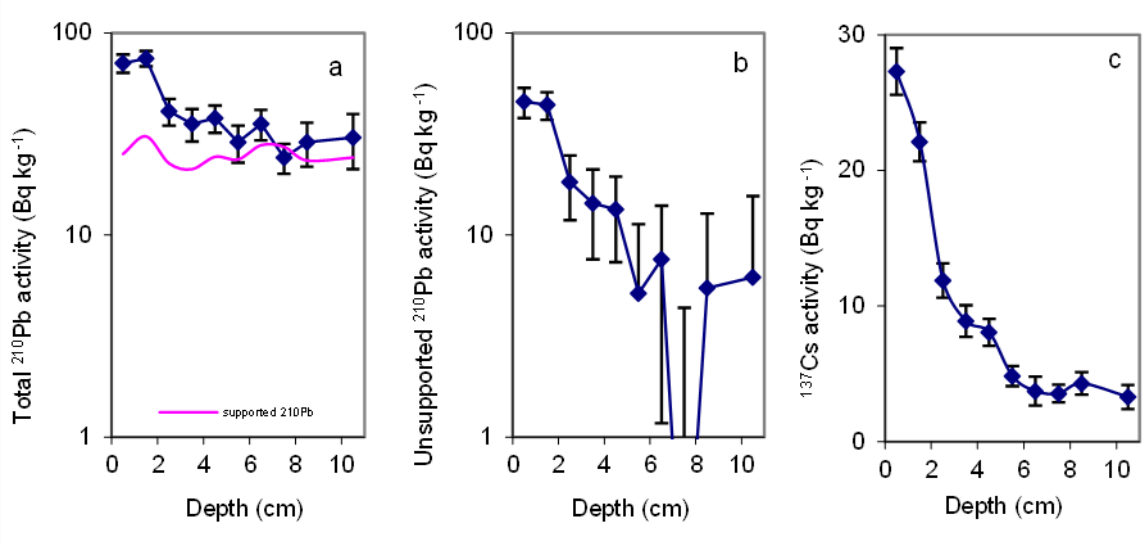

Fig. 5. Fallout radionuclide concentrations showing a) total ^{210}Pb, b) unsupported ^{210}Pb and c) ^{137}Cs concentrations versus depth.

The samples dated by radiocarbon range in age from 960 cal BP to 7300 cal BP (Table 1). One age reversal occurs between the two lowermost samples, but the remaining eight dates yielded consistently younger ages. The accumulation rate is relatively high in the lowermost part of the sequence, between 7400 and 7000 cal BP, and relatively low between 7000 and 5000 cal BP. Since 5000 cal BP the accumulation rate has been relatively constant.

Table 1. Radiocarbon data obtained from the Red-throated Loon Lake core.

Sample ID	***Lab no.***	***Depth below sediment surface (cm)***	***Material***	***Reported age (^{14}C yr BP)***	***Individually calibrated age (mid-intercepts) (cal BP)***	***Individually calibrated age (2σ interval)(cal BP)***
RTL209	LuS17326	29-31	4 *Salix* leaves, 14 unidentified leaf fragments	1080±30	969	928-1058
RTL219	LuS17327	49-51	6 *Dryas* leaves, 3 *Salix* leaves, 1 twig, 12 unidentified leaf fragments.	1815±30	1745	1621-1821
RTL230	LuS17328	71-73	5 *Dryas* leaves, 1 *Salix* leaf, 2 twigs, 11 unidentified leaf fragments.	2525±35	2634	2491-2744
RTL241	LuS18279	93-95	1 *Dryas* leaf, 2 pieces of bark, 1 unidentified leaf	3335±30	3559	3469-3680

RTL249	LuS18280	109-111	19 *Dryas* leaf fragments, 40 unidentified leaf fragments	3805±30	4217	4089-4345
RTL256	LuS18281	123-125	15 *Dryas* leaf fragments, 2 twigs	4275±30	4849	4730-4954
RY19-5-R-8-909-911	LuS17078	134,5-136,5	20 *Dryas* and *Salix* leaf fragments, some unidentified twigs	4765±40	5506	5329-5589
RTL266	LuS18282	143-146	10 *Dryas* leaf fragments, 19 unidentified leaf fragments	5470±35	6284	6198-6386
RTL273	LuS18283	164-167	2 *Dryas* leaves, 2 pieces of bark, 2 unidentified seeds, 4 unidentified leaf fragments	6380±45	7293	7171-7423
RY19-5-R-8-954-951	LuS17077	176-181	30 *Dryas* and *Salix* leaf fragments	6335±45	7261	7162-7417

3.2 Sediment description and macrofossils

The sediment sequence measures 186 cm in total and can be divided into two main units. Unit 1 spans the lowermost 51 cm of the sequence and unit 2 the uppermost 135 cm (Fig. 6). The two units have a gradual contact. Unit 1 is composed of a light brownish grey clay with very low total organic carbon (TOC) (<1%). The clay has darker laminations as well as horizons rich in organic detritus. The lowermost 3-4 cm of unit 1 consists of course sand and gravel. The elemental C/N ratio varies greatly between different samples. Unit 2 is composed of a greenish light brown gyttja with TOC up to 15% (Fig 6). The unit has several dar-

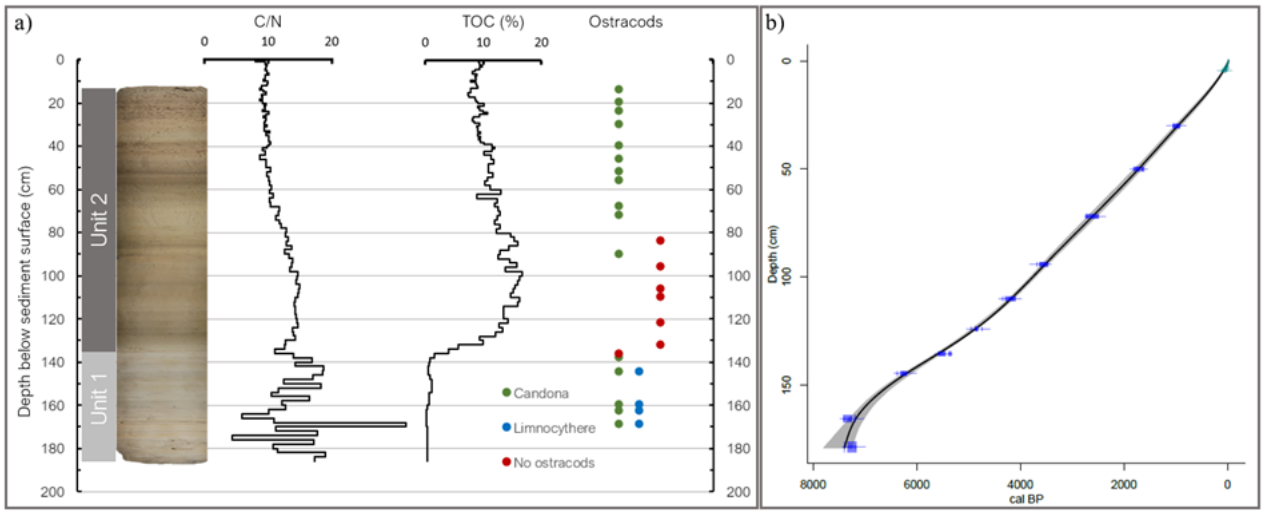

Fig. 6. a) Core stratigraphy of Red-throated Loon Lake including a photograph of the sediment sequence and depth profiles of the C/N ratio, TOC content and presence of ostracods. b) Age-depth model based on ^{14}C, ^{210}Pb and ^{137}Cs ages.

ker bands, and the top is relatively rich in organic detritus. The content of TOC decreases towards the top. The C/N ratio is more stable than in Unit 1 and decreases steadily from a depth of 100 cm and upwards. The unit contains both quartz and carbonate sand grains.

Small light green transparent spheres of varying sizes, from approximately 2 mm to 8 mm in diameter, can be found throughout the sediment sequence and are interpreted to be fish eggs (Fig. 7). They appear to be most abundant around a depth of 110 cm.

Ostracods are present in the lower part of the core (below ~138 cm) and belong to the genera *Candona* and *Limnocythere* (Fig. 7). No ostracods were observed between the depths of 90 and 138 cm. The ostracods above 90 cm belong exclusively to the genus *Candona*. Insect remains are abundant throughout the core. Intact leaves are mostly identified as *Dryas integrifolia* and are relatively abundant, except for in the uppermost 40 cm. Leaves of *Salix arctica* were also identified but occur to a lesser extent. Moss remains occur throughout the core but are most abundant closer to the top.

3.3 Elemental geochemistry

Si, Mn and S were in general not as well counted as the other elements. The profiles of Si, K, Fe, Ti, and Rb all show similar profiles in general (Fig. 8). K and Si show a strong positive correlation, as do Ti, Rb and Fe (Appendix A). The profiles of Ti, Fe and Rb increase from around 6500 cal BP until 5500 cal BP, after which they remain relatively constant until about 3800 cal BP (Fig. 8). K and Si reach a peak slightly earlier, around 6200 cal BP. Around 3500 cal BP K, Ti, and Fe show transient decreases. By 3000 cal BP, Rb decreases to a slightly lower level while Fe shows a short-lasting peak. Si shows a minimum around 3500 cal BP. The profiles of Si, K, Ti, Fe, Rb and Mn all show minor peaks around 1200 cal BP.

The profiles of Br and S show an increasing trend to-

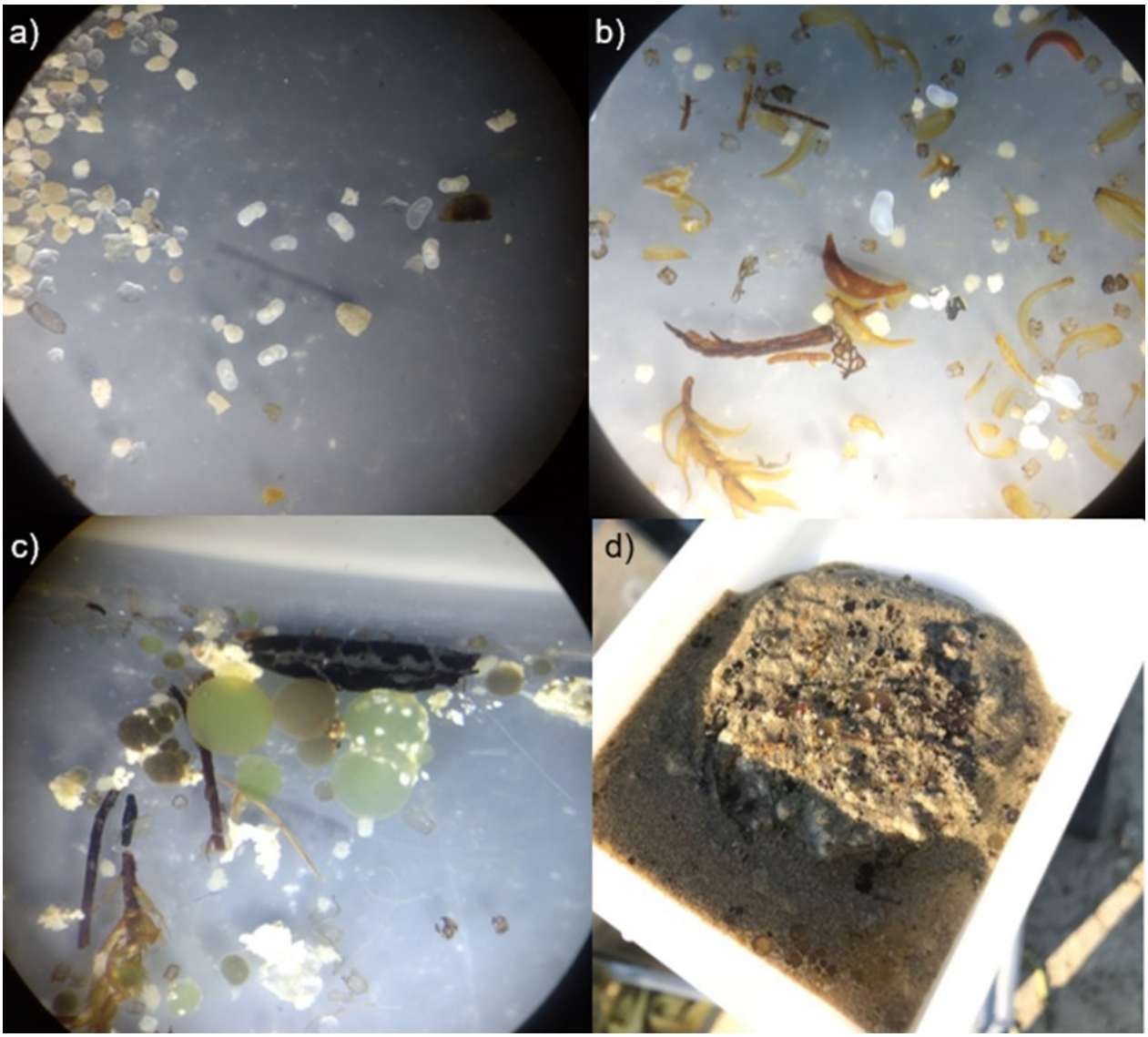

Fig. 7. a) Photo of ostracods from the genus Limnocythere from a stereoscope with the magnification set to 50x, b) Ostracods from the genus Candona, c) Transparent spheres interpreted to be fish eggs. d) Photo of sediment from the gravity core, showing the same type of transparent spheres as in c).

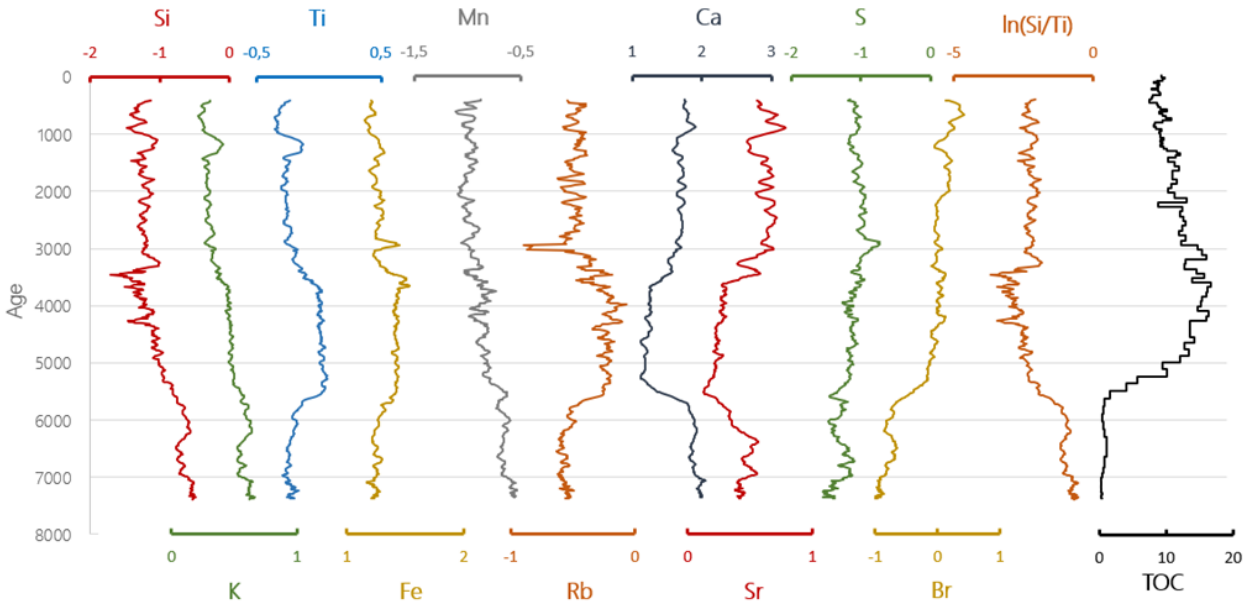

Fig. 8. Profiles of CLR-transformed XRF data, as well as ln(Si/Ti) and TOC (%), plotted against age (cal BP).

wards present, and are relatively low before 6000 cal BP, followed by increase until about 5300 cal BP. Br increases slightly more just before 2000 cal BP and shows a transient minimum around 1200 cal BP while a maximum occurs around 700 cal BP.

The profiles of Ca and Sr look very similar to each other, and they show a strong positive correlation (r=0.81). These two records show a slight decrease from 7300 to 6000 cal BP, followed by rapid decrease. Between 5500 and 3700 cal BP the Ca and Sr profiles remain stable, after which they show increasing trends until about 3000 cal BP. For the last 3000 years they remain fairly stable with a slight transient decrease around 1200 cal BP and minor peaks at about 1000 cal BP, similarly to Br. Ca show a positive correlation with Si and K in unit 1, and a negative correlation in unit 2.

The ratio of Si/Ti is relatively high before 6000 cal BP. During a period of a few hundred years, it decreases relatively rapidly. The ratio is low between 5400 cal BP and 3400 cal BP, after which it increases abruptly and then remains stable towards present.

3.4 Pollen

The number of counted pollen grains per sample is generally low, and ranges from 2 to 46 (Appendix B). The total number of counted pollen grains is 301. The number of counted pollen is generally higher before 6000 cal BP. 10 types of pollen were identified (Fig. 9). The pollen percentage diagram shows that *Salix* and Cyperaceae are the two dominating pollen types (Fig. 10). Before 6000 cal BP *Salix* constitutes about 90% of the counted pollen. The apparent increase in Cyperaceae after 6000 cal BP is mainly a result of the decreasing amount of *Salix* since the influx of Cyperaceae only increases slightly (Fig. 11). Overall, interpretations of changes in pollen percentage and influx should be applied with caution due to the low number of counted pollen.

Salix is the only pollen type that occurs in every sample. The total influx of pollen is generally less than 10 grains/cm^2/year (Fig. 11). The influx of *Salix* decreases from the beginning of the sequence until around 6000 cal BP, after which it remains stable until present. The *Salix* pollen grains in the lower part of the sequence are generally more deformed and smaller than *Salix* grains higher up in the sequence. The influx of Poaceae and *Saxifraga* is low and relatively stable. *Saxifraga* does not occur before 6300 cal BP and the influx of *Saxifraga* is highest at around 1000 cal BP, where it comprises about 40% of total pollen influx. Polypodiaceae spores occur in four samples and constitute about 60% of all palynomorphs (pollen and spores) in one sample.

Pollen of four tree taxa were found, and they comprise a relatively small portion of the pollen counts. Pollen of *Ulmus* and *Betula* were found in one sample, respectively. Two samples contained pollen of *Alnus* and four samples contained pollen of *Pinus*. The numbers of counted tree pollen are too low to discern any trends.

Pollen of Caryophyllaceae were identified in one sample, and pollen of Brassicaceae were found at four depths, and constitute almost 30% of the counted pollen in one sample. *Sphagnum* spores occur in three samples. The influx of unidentified spores varies greatly but is generally higher than 1,000 spores/cm^2/year, and are due to their relative abundance not included in the pollen precentage diagram (Fig. 10). The influx seems to be higher in the beginning, end, and middle of the record. The unidentified spores are likely from either moss, fungi, or algae. Single spores of *Sporormiella* were recorded at ~2000, ~3000, and ~3300 cal BP.

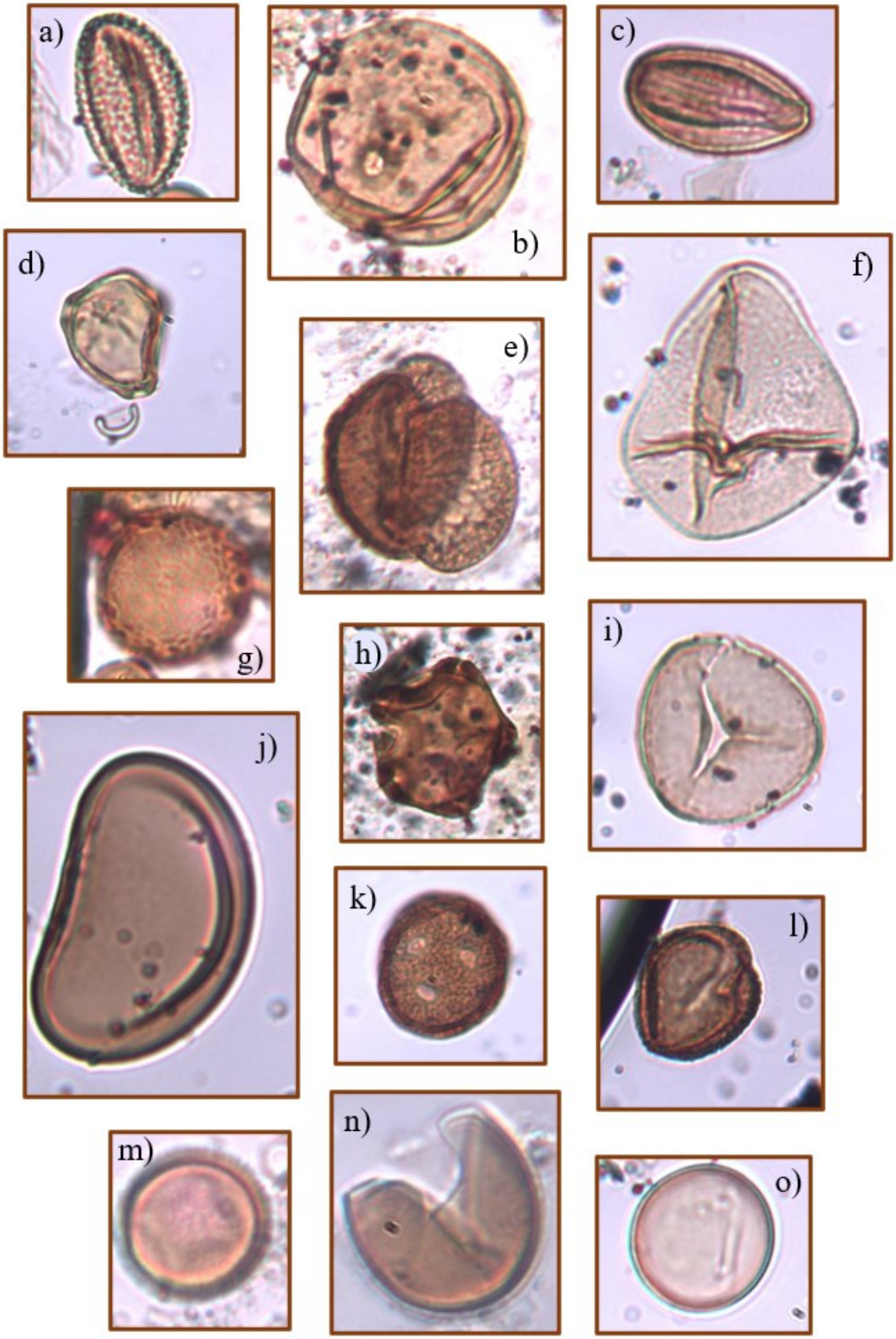

Fig. 9. Pollen and spore types; a) *Salix* b) Poaceae c) *Saxifraga* d) *Betula* e) *Pinus* f) Cyperaceae g) *Ulmus* h) *Alnus* i) *Sphagnum* j) Polypodiaceae k) Caryophyllaceae l) Brassicaceae m) Unidentified spore n) Unidentified spore o) Unidentified spore

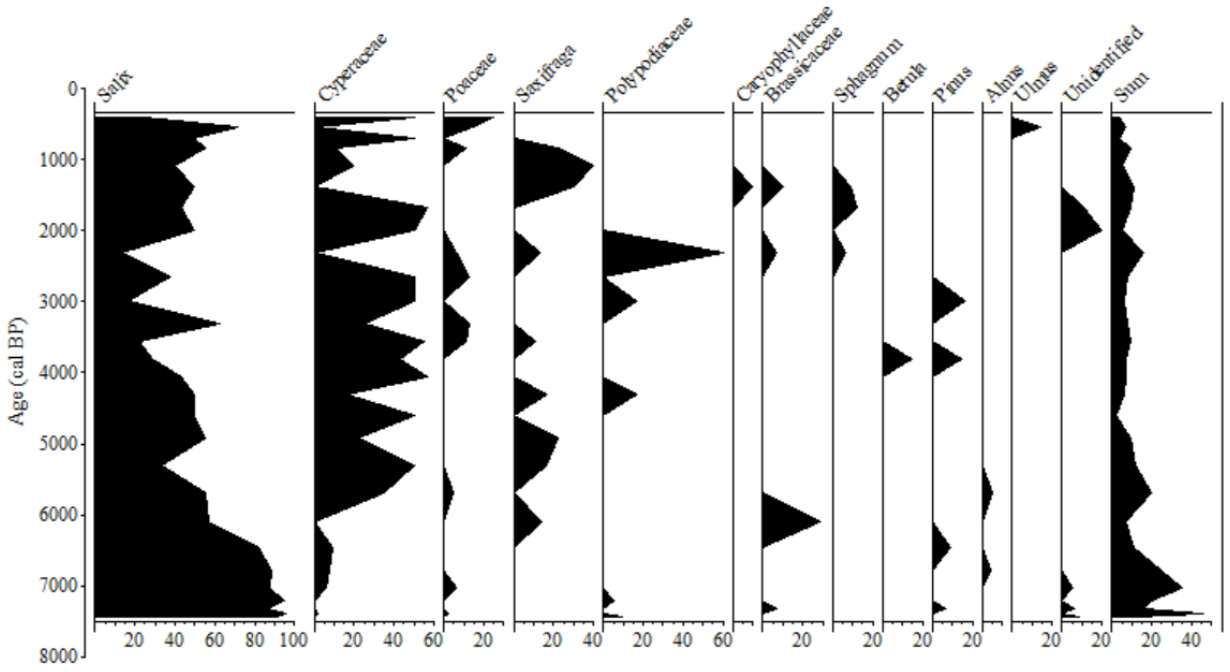

Fig. 10. Pollen percentage diagram of Red-throated Loon Lake presented as percentages of each taxon. The Sum graph shows the total amount of counted pollen as well as Spaghnum and Polypodiacae spores.

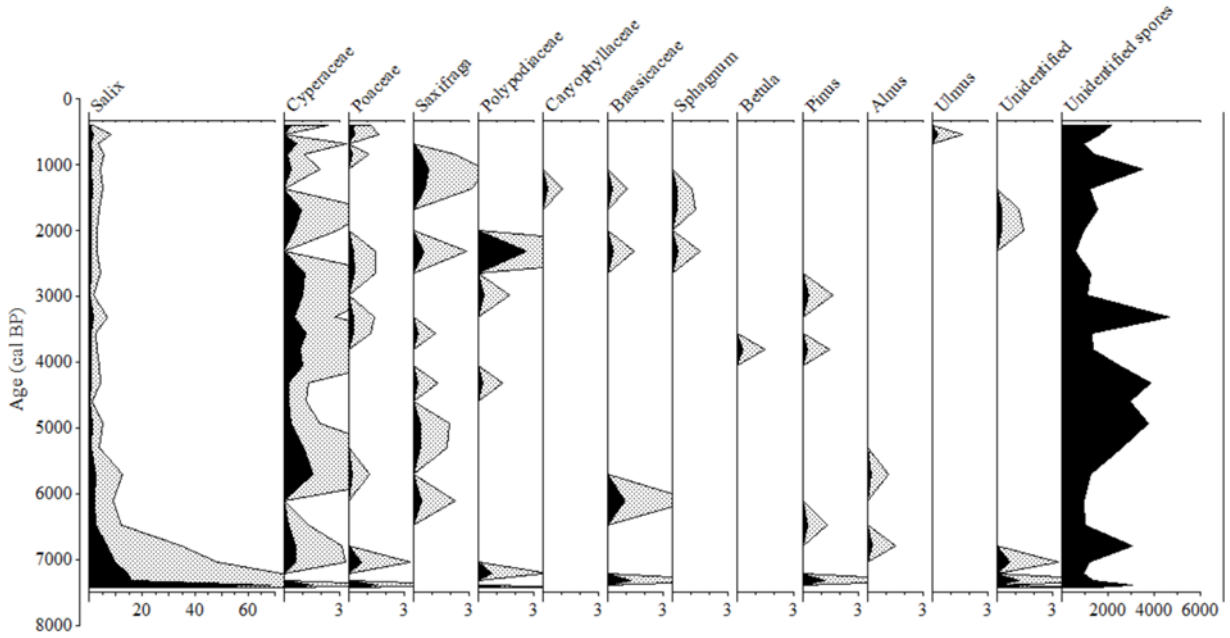

Fig. 11. Influx of pollen and spores presented as number of grains/cm^2/year, with an exaggeration of 5x.

4 Discussion

4.1 Deglaciation

The lowermost sediments, containing gravel, were likely deposited relatively close to the ice sheet and thus one can assume that the sediment sequence spans the entire period during which the site has been deglaciated. Thus, the approximate time of deglaciation of Red-Throated Loon Lake is sometime just before 7300 cal BP. According to Bennike (2002) the minimum age of deglaciation of north-western Washington Land is 7800-7900 cal BP and for south-western Washington Land 7500-7600 cal BP, which fits well with the lake sediment data. Since a return of the ice sheet would likely result in deposition of courser sediments similarly to those at the base of the sequence (Axford et al., 2019), it is unlikely that the ice sheet returned to Red-Throated Loon Lake after the deglaciation.

There is a general lack of consensus regarding the timing of the deglaciation in the terrestrial parts of northern Greenland. England (1985) has studied Hall Land, northeast of Washington Land on the western side of the Petermann Glacier and claims that deglaciation was initiated no earlier than 8300 cal BP and was completed by 6200 cal BP. However, Bennike et al. (1987) argue that the deglaciation of Hall land started at 10,000 cal BP at the latest.

Two relatively recent studies have reconstructed the retreat of the ice margin in Nares Strait, both of which have taken the dates from Bennike (2002) into account. Dalton et al. (2020) claim that large parts of Washington Land were deglaciated already by 10,300 cal BP. According to Georgiadis (2018) Washington Land was, apart from a strip along the coastlines, covered by ice as late as 7500 cal BP (Fig. 12). My data thereby shed new light on the deglaciation of Washington Land.

It is, however, possible that the GrIS had retracted from Red-Throated Loon Lake earlier than 7300 cal BP, and that the area had until the inferred date of deglaciation been covered by a local glacier, since Washington Land has several smaller ice caps. A study of the Qaanaaq ice cap in north-western Greenland suggests that it was significantly smaller during parts of the Holocene, but since then it has almost fully readvanced and reached its pre-Holocene extent (Søndergaard et al., 2019). Any studies dealing with the former extent of glaciers in Washington Land do not seem to exist.

4.2 Vegetational history

The low influx of pollen is consistent with the present airborne pollen influx measurements from Greenland (Porsbjerg et al., n.d.), as well as inferred past influx from other palaeoecological studies in the region (Hyvärinen, 1985).

The dated leaves of *Salix* and *Dryas* that yielded an age of 7300 cal BP prove that these species were established in the catchment very soon after the deglaciation. Studies of recently exposed glacier forelands in Greenland and High Arctic Canada show that *Salix* established quickly after retreat of the glaciers (Boulanger-Lapointe et al., 2014), which explains the relative abundance of *Salix* pollen even in the samples from the bottom of the sequence (Hyvärinen, 1985).

There are few pollen records from northern Greenland, and those that exist are almost exclusively from the north-eastern parts (Fredskild, 1995; Funder & Abrahamsen, 1988; Jakobsen et al., 2008; Wagner et al., 2000). The nearest lakes with a pollen record are

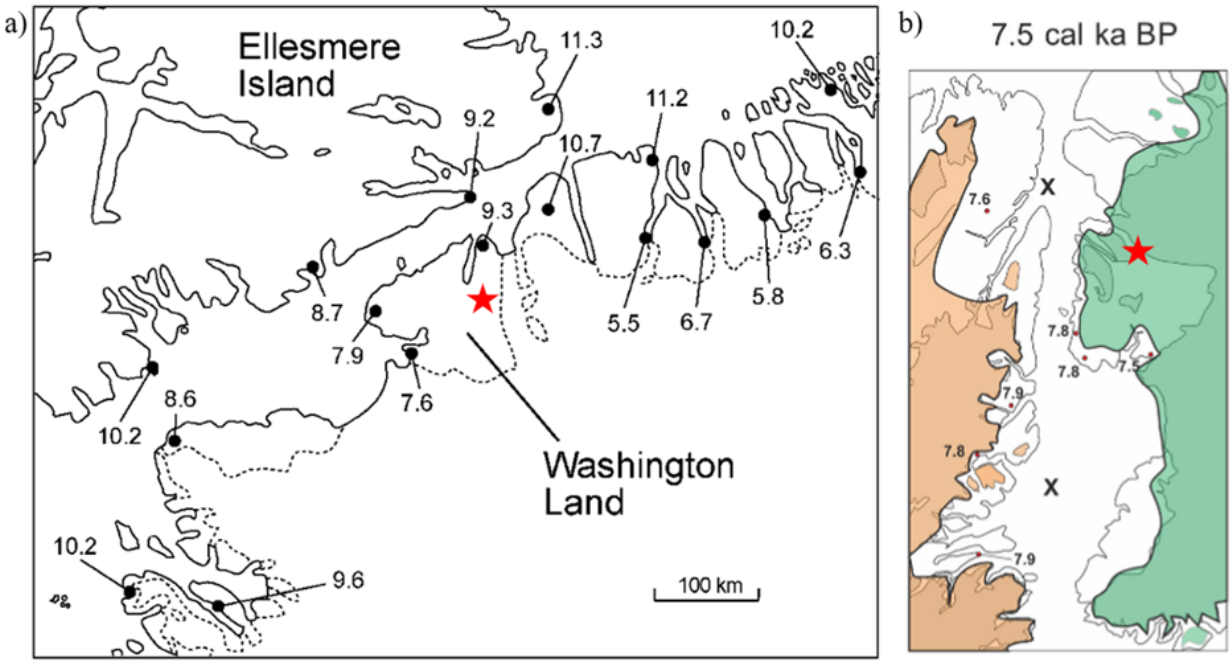

Fig. 12. Map of the Nares Strait region with calibrated ages indicating the minimum timing of deglaciation. The location of Red-Throated Loon Lake is marked with a red star. a) From Bennike (2002). b) Reconstructed ice margin of the Innuitian and Greenland Ice Sheets from Georgiadis et al. (2019), based on data from England (1999), Bennike (2002), Jennings et al. (2011) and Jakobsson et al. (2018).

Kap Inglefield Sø in Inglefield Land, southwest of Washington Land (Blake et al., 1992), and Klaresø in Peary Land, northern Greenland (Fredskild, 1973)(Fig. 13). Klaresø is situated on a lower altitude and was inundated by the sea until approximately 5600 cal BP. Here, *Salix* became the dominant species after 5500 cal BP. The high amount of deformed and flattened *Salix* pollen grains in the clayey sediments (unit 1) of Red-Throated Loon Lake corresponds well to Blake et al. (1992) who ascribes the deformation to transport with meltwater rich in sand and mud.

The pollen record from Kap Inglefield Sø extends from sometime before 8000 cal BP until ~4500 cal BP. Its most prominent feature is the exceptional abundance of *Salix* pollen between 8000 and 7000 cal BP. The trend of *Salix* is consistent with my record. *Salix* is not abundant in the lowermost part of Klaresø sediment sequence, but it is likely that the peak of *Salix* in my record occurred prior to the beginning of that recorded of Fredskild (1973). High abundances of *Salix* around 7000 cal BP have been reported from other areas in northern Greenland as well as Ellesmere Island (Hyvärinen, 1985; Kusch et al., 2019; Wagner & Bennike, 2015). Blake et al. (1992) identified the majority of the *Salix* pollen grains to belong to *Salix arctica*, and only two to belong to *Salix herbacea*. Since *Salix arctica* currently grows in Washington Land it is reasonable to believe that they comprise a majority of the *Salix* pollen from Red-Throated Loon Lake.

Fig. 13. Map of Greenland. Klaresø is situated in Peary Land north-east of Washington Land (Fredskild, 1973, and Kap Inglefield Sø in Inglefield Land south-west of Washington Land (Blake et al., 1992).

Spring (~June) snow cover is the main limiting factor for growth of *Salix arctica* in Greenland, whereas temperature seems to have little to no effect (Schmidt et al., 2006). However, snow is crucial for the survival of *Salix arctica* since melting of thick snow cover creates a supply of water during the summer months (Boulanger-Lapointe et al., 2014). The relatively constant levels of *Salix arctica* during the last 6000 years may indicate a relatively constant duration of the snow-free season, without any longer periods of decreased or increased snow cover.

Cyperaceae is most abundant between ~7000 and ~4700 cal BP in Kap Inglefield Sø (Blake et al., 1992) and between 5500 and 2000 cal BP in Klaresø (Fredskild, 1973). The trend in Kap Inglefield Sø is at least somewhat similar to that in Red-Throated Loon Lake. F. Dalerum et al. (unpublished data) identified *Carex nardina* as the only member of the Cyperaceae family in Washington Land, and therefore it is likely that most of the pollen grains identified as Cyperaceae belong to the species *Carex nardina*, which usually grows in very cold and windy locations, preferably on carbonate-rich bedrock (ArtDatabanken, n.d.).
Polypodiaceae is expected to be found even in the lowermost parts of the sediment sequence since it was one of the first taxa to colonize Greenland after the deglaciation. However, the relatively high abundance in just one single sample is surprising, and may be the result of the remains of an individual plant or sporangium washed into the lake (Björck et al., 1994).

The tree pollen is interpreted to be long-distance pollen. *Ulmus* and *Pinus* do not occur in Greenland at present, *Alnus* is not native to northern Greenland (Fredskild, 1995), and *Betula* can only be found on the eastern and western coasts of Greenland (Fredskild, 1991). How, and more importantly from where, the long-distance pollen is transported is difficult to assess, given the variability as well as the insufficient understanding of the movement of atmospheric air masses over Greenland (Rousseau et al., 2008). However, a majority of the long-distance pollen is most likely from Canada (Porsbjerg et al., 2003).

The tree pollen could also originate from an earlier interstadial or interglacial when trees grew in northern Greenland. The earlier marine part of the pollen record from Klaresø (Fredskild, 1973), pre-5600 cal BP, is dominated by taxa such as *Betula* and *Alnus*, and likely redeposited pollen were abundant in the lower minerogenic unit of Kap Inglefield Sø (Blake et al., 1992). The same trend has been reported from Ellesmere Island (Hyvärinen, 1985). This trend cannot be recognized in Red-Throated Loon Lake as the influx of tree pollen is both minimal and sporadic.

4.3 Environmental history

The low content of TOC in the clayey sediments of unit 1 indicates a relatively unproductive lake and catchment. The C/N ratio variations likely reflect very low contents of nitrogen as well as varying sources of organic matter since higher values indicate terrestrial input whereas sediment with values between 4 and 10 can be interpreted as derived mainly from algae (Meyers, 2003). The dominance of clay after the initial

layer of gravelly sand indicates that no major streams carried meltwater to the lake since that likely would have resulted in higher influx of courser material. However, the ice margin may have been situated relatively close to the lake during the first millennia of the lake history.

Br is mainly associated with organic matter (Fuge, 1988), and the upwards increasing trend of both TOC and Br that starts around 5800 cal BP is interpreted as an increase in lake productivity. Since bromine is often incorporated into the organic component of algae it is mainly autochthonous and an increase in Br can be used as a proxy for warming (Fedotov et al., 2012; Kalugin et al., 2013; Phedorin et al., 2000). Soil organic matter is also enriched in bromine and elevated amounts could be due to weathering of humus-rich soil or peat (Oldfield et al., 2003), and leaching of soils likely also cause the increase in S (Olsen et al., 2013). Axford et al. (2013) recorded maximum organic matter content associated with warming between 6200 and 4200 cal BP at Loon Lake, western Greenland, which is consistent with my increase in organic content in Red-Throated Loon Lake. The influx of Cyperaceae is slightly elevated during this approximate time span.

Si, K, Ti, Fe, and Rb are generally considered to represent the lithogenic fraction of the sediment. Si could represent deposition of biogenic silica, but since the Si and K records show a strong correlation that is likely not the case (Davies et al., 2015). Both Si and K have their maxima in unit 1 when the lake was supposedly still relatively close to the ice sheet. Ti is often used to track changes in catchment hydrology, such as precipitation and runoff (Haug et al., 2001; Peterson et al., 2000). Ti, unlike Fe, is not sensitive to redox conditions and it provides a more reliable proxy (Yarincik et al., 2000). However, Fe, as well as Rb, correlate well with Ti ,while Mn correlates well with Si, and they are all interpreted to reflect minerogenic input (Czymzik et al., 2010; Kalugin et al., 2013; Kylander et al., 2011).

Since the profiles of Si and K decrease from unit 1 to unit 2, while Ti, Fe and Rb increase, it is likely that the catchment experienced a change. Since Axford et al. (2013) recorded warming during this approximate time, the change may be related to an increase in chemical weathering. Ti is also primarily associated with the finer sediments, such as silt and clay, while Si often composes the courser fraction (Cuven et al., 2010; Kylander et al., 2011). The Si/Ti ratio can therefore be interpreted to represent grain size (Shala et al., 2014). The decrease in Si/Ti in the top of unit 1 likely reflects a decrease in grain size, which together with the gradual transition from clay to gyttja is interpreted as the result of the ice sheet moving away from the lake and onset of warmer conditions (Striberger et al., 2012).

The C/N ratio follows the trends of both the lithogenic elements (K, Si, Ti, Fe & Rb) and TOC content and in unit 2 reaches a maximum close to the base. Since the C/N ratio exceeds 10 the organic matter is likely dominated by terrestrial carbon, and it is likely that an increase in runoff caused a more continuous input of terrestrial plant matter. However, elevated C/N ratios may also be related to nitrogen deficiency, and algae limited in N can have C/N ratios considerably higher than the common 7-8 (Talbot & Lærdal, 2000). Many lakes in Greenland are relatively oligotrophic. The C/N ratio reached a maximum during the mid-Holocene warm period, and although soil-derived carbon and terrestrial organic matter may have contributed, a limitation of N due to increased productivity could account for the generally low N content of the sediments (Bergström et al., 2008).

Ca and Sr can represent both detrital input and authigenic or biogenic calcium carbonate minerals (Davies et al., 2015; Koinig et al., 2003). The overall stratigraphy of Red-Throated Loon Lake closely mimics that of Trifna Sø (Kusch et al., 2019), and Lille Sneha Sø (Wagner & Bennike, 2015), both in the Skallingen area, eastern north Greenland. The three lakes show similar trends in regard to biostratigraphy and TOC and Ca. The decrease in Ca after 6000 cal BP in my record corresponds well with the increase in productivity inferred from the Br and TOC records, and while Br continues to increase, TOC decreases when Ca increases. Previous research indicates that TOC and carbonates can have negative relationships in lacustrine sediments. Wagner and Bennike (2015) recorded relatively high contents of Ca as well as Total Inorganic Carbon (TIC) in the bottom of their sediment sequences (Fig. 14), followed by very low values

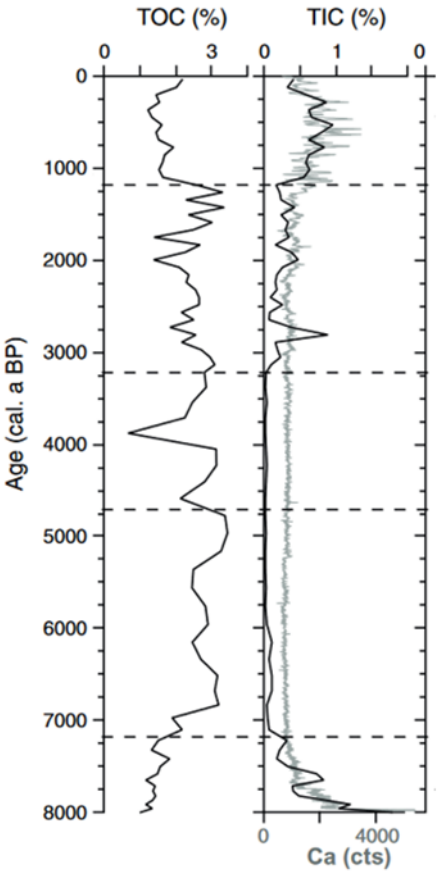

Fig. 14. Elemental geochemistry of Lille Sneha Sø. Profiles of total organic carbon (TOC (%)), total inorganic carbon (TIC (%)) and Ca (counts per second) plotted against age. From Wagner and Bennike (2015).

during the mid Holocene and slightly higher during the late Holocene, similar to how Ca varies at Red-Throated Loon Lake. Kusch et al. (2019) found a similar trend in TIC. However, Wagner & Bennike (2015) interpret the increase in Ca as an increase in detrital input since it correlates with K in their sequence. Ca does have a positive correlation with K as well as Si in unit 1 in my record, before 5500 cal BP, similarly to Wagner & Bennike (2015), and Ca is aften associated with detrital input in glacial environments (Davies et al., 2015).

However, changes in detrital input likely do not account for the Ca variations in unit 2, as Ca has a negative correlation with Ti, Fe and Rb, and no correlation with K or Si. Thus, Ca in the sediments likely has more than one source (Cuven et al., 2011).

The trend of Ca is also intriguing when compared to the presence versus absence of ostracods in the sequence, and there are several potential explanations. The period of low Ca corresponds very well with the interval without any preserved ostracods (Fig. 6), and the supply of Ca might have been too low for the ostracods to build their shells. Both ostracod genera in the sediment sequence can be found in Greenland and the ostracods in my record likely belong to species adapted to arctic conditions (Bennike, 2000; Bunbury & Gajewski, 2009). The shift towards warmer and otherwise more productive conditions might have been unfavourable for the ostracods.

Alternatively, poor preservation due to dissolution could explain the trend of both Ca and ostracods. During times of high production in a stratified lake the decomposition of organic matter could lower pH enough to dissolve deposited or precipitated CaCO3. If the sediment contains 12% or more organic carbon little to no carbonates are preserved (Dean, 1999). Since the TOC content remains higher than 12% between 5500 and 3000 cal BP in Red-Throated Loon Lake, dissolution could at least partly explain the low Ca content and absence of ostracods. It has been shown that newly exposed lakes follow a general trend of increased productivity. Mineral weathering from newly exposed soil cause nutrient loading followed by a decline in pH (Engstrom et al., 2000).

Based on the discussion above, the period between 5500 and 3500 cal BP may have been the most productive and thereby warmest. Yet, Olsen et al. (2012) state that the HTM of northern Greenland lasted between 7200 cal BP and 6500 cal BP and Bennike & Wagner (2015) inferred maximum warming at about 7000 cal BP for north-eastern Greenland, at a time when Red-Throated Loon Lake was dominated by minerogenic sedimentation. Since close proximity to an ice sheet has been claimed to delay onset of HTM conditions (Kaufman et al., 2004), a viable hypothesis for the late HTM in Washington Land might be its relative proximity to the GrIS. The ice sheet and valley glaciers extended further in north-western Greenland than in the relatively dry northern tip of Greenland, thereby covering the land for longer and prolonging glacial conditions. According to Bennike (2002) the ice margin of the Humboldt Glacier was likely only 25 km behind its present position during the HTM. Organic sedimentation will dominate when the catchment is deglaciated and no longer fed by glacial meltwater (Balascio et al., 2013), and even though the catchment in this case is very limited in size, Red-Throated Loon Lake was likely fed by meltwater to some degree before 5500 cal BP, likely in combination with fluvial erosion. Sediment in suspension likely impacted the lake ecology, reducing the ability of sunlight to penetrate the water column and thereby stalling the growth of algae. When soil formation and an increase in vegetation cover resulted in less catchment erosion, chemical weathering became relatively more important (Giguet-Covex et al., 2011), and less sediment in suspension resulted in increased productivity.

Just like in Red-Throated Loon Lake a decrease in TOC content was detected in Kap Inglefield Sø during the latter half of the Holocene (Blake et al., 1992). Both Kap Inglefield Sø and Klaresø experienced decreased sedimentation rates after ~4500 cal BP, something that Blake et al. (1992) explained by an increase in duration of the seasonal ice cover of the lake. This trend was not observed in Red-Throated Loon Lake, and either the seasonal ice cover remained stable, or the decrease in sedimentation rate was compensated for by other processes. Axford et al. (2013) recorded an abrupt cooling event at 4200 cal BP. This is not recognized in Red-Throated Loon Lake where the inferred cooling appears rather gradual. The dip in Si around 3500 cal BP lacks a counterpart in the other profiles and is likely due to poor detection of Si by the scanning XRF. All of western Greenland experienced colder and drier conditions after 4000 cal BP, related to neoglacial cooling (Presthus Heggen et al., 2010). Between 3200 cal BP and 2100 cal BP the GrIS advanced once again (Farnsworth et al., 2018). The reconstructed temperature of north-western Greenland correlates well with the decline of summer insolation during the Holocene (Fig. 15) (Axford, 2019).

4.4 Late Holocene

After 3000 cal BP the profiles of the lithogenic elements (Si, K, Ti, Fe and Rb) all show similar short-term trends. The profiles of Br, Sr and Ca, as well as TOC show the inversed trend of the lithogenic elements, which indicates that Ca on this timescale could be related to changes in productivity rather than in detrital input. The minerogenic input seems to be relatively consistent between 3000 and 2000 cal BP, whereas the productivity based on Br seems to increase slightly around 2000 cal BP and stays high until 1400 cal BP. This period is known as the Roman Warm Period (RWP) and was generally warm (Ljungqvist, 2010), although evidence suggests large variabilities on a regional scale. Reconstructions of the GrIS suggests cold temperatures (Dahl-Jensen et al., 1998) whereas Canada experienced warm and wet conditions (Holmquist et al., 2016). Since no signs of an increase in runoff can be inferred from the Red-Throated Loon Lake sediments, nor a clear increase in TOC, the climate of Washington Land was likely not that warm or wet during the RWP, however the Neoglacial cooling was likely halted.

Most of the profiles show a relatively abrupt change around 1400 cal BP. The lithogenic elements peak in ~1200 cal BP, while Br, S, Sr and Ca decrease. During this time TOC is relatively low and C/N remains constant. The core is relatively light in colour

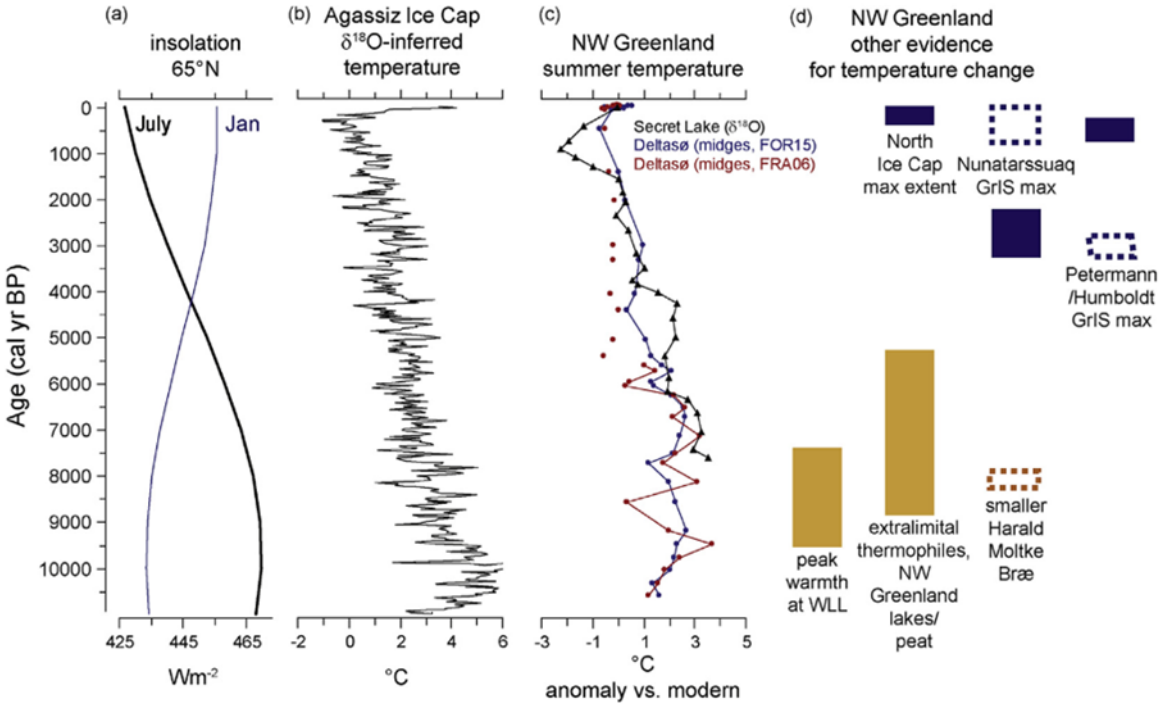

Fig. 15. From Axford et al. (2019) and references therein a) insolation at 65°N during July and January b) Temperatures inferred from δ18O of ice at Agassiz Ice Cap, Ellesmere Island c) modelled July air temperature anomalies at Deltasø based on chironomid data (red and blue) and chironomid δ18O-inferred summer temperature anomalies from nearby Secret Lake d) Other evidence for air temperature changes over northwest Greenland.

and contains less macrofossils. Based on all this evidence, this is interpreted as a cold event. The positive peak in lithogenic elements may be interpreted as increased aeolian deposition due to more arid conditions or can be a result of decreased dilution by organic sedimentation (Axford et al., 2013). This peak corresponds well with the Dark Ages Cold Period (DACP) (Helama et al., 2017). During this time western Greenland supposedly experienced warmer sea surface temperatures and less extensive sea ice (Ribeiro et al., 2012), and the north Atlantic experienced the warmest period during the late Holocene (Moros et al., 2012).

An increase in productivity after 1000 cal Bp, inferred from the TOC and Br records, indicates that Red-Throated Loon Lake likely experienced warmer conditions. Lake records in southern and western Greenland also show increased productivity around 1000 cal BP (Kaplan et al., 2002; Olsen et al., 2013) which corresponds with the Medieval Warm Period (MWP). The MWP lasted from 1100 cal BP until 600 cal BP and is characterized by increased summer temperatures in various parts of the world, including northern Europe and southern Greenland, however there are inconsistencies and contradictions regarding the timing and extent (Hughes & Diaz, 1994; Lamb, 1965). Southern Greenland experienced clearly elevated sea surface temperatures and a minimum in sea ice (Miettinen et al., 2015). Temperature reconstructions based on oxygen isotope records from ice cores from the GrIS, as well as temperature reconstructions based on marine sediments indicate elevated temperatures of land and sea, respectively (Andresen et al., 2011; Dahl-Jensen et al., 1998). At the same time glaciers of western Greenland were advancing and reached maxima towards the end of a proposed MWP (Jomelli et al., 2016; Young et al., 2015). Dinoflagellate and marine diatom assemblages indicate lower sea surface temperatures and more sea ice in western Greenland during the earlier MWP (Krawczyk et al., 2010; Ribeiro et al., 2012). Temperature reconstructions based on pollen also record elevated temperatures in the western and central Arctic around 1000 cal BP, although no significant change is seen in Greenland (Gajewski, 2015). Red-Throated Loon Lake shows slightly elevated levels of *Saxifraga* and unidentified spores during this time, which could indicate warmer conditions.

The very top part of the profiles (Fig. 9) shows an increase in the lithogenic elements and a decrease in Br and TOC, indicative of relatively cold and less productive conditions. O´Brien (1995) records abrupt onset of colder conditions 600 cal BP, which is associated with the Little Ice Age (LIA). The LIA in Greenland was characterized by glacier expanse that culminated by around 400 cal BP (Kjær et al., 2022).The Petermann Ice Tongue reached its neoglacial maximum extent 600 cal BP (Reilly et al., 2019). A small increase in TOC is recorded during the last few hundred years. However, as the uppermost sediments were not studied with XRF analysis, it is difficult to draw any conclusions about recent climate development in Washington Land.

4.5 Potential implications for palaeogenetic studies

It has been shown that pollen and macrofossil analysis combined with palaeogenetic analyses can provide more detailed information about past vegetational changes, especially in high arctic environments that have overall little vegetation but provide excellent conditions for the preservation of sedimentary ancient DNA (Epp et al., 2015; Pedersen et al., 2013). One method used to achieve this is called DNA metabarcoding, through which a section of the chloroplast genome is compared to already available reference databases (Taberlet et al., 2006). Palaeogenetic analysis of a sediment sequence from northernmost Greenland reveals that *Salix*, *Poaceae*, *Empetrum* and *Saxifraga* were present as early as 10,800 cal BP (Epp et al., 2015).

According to Bennike (2002) the mammal fauna of northern Greenland is and has been fairly limited. Musk-ox (*Ovibos moschatus*) likely immigrated from Ellesmere Island during the mid-Holocene (Bennike & Andreasen, 2005). Humans also immigrated to northern Greenland during approximately the same time. However, recent studies suggest that humans might not have been the main control of the population dynamics of musk-ox. Instead, environmental change likely played an important role (Campos et al., 2010). *Sporormiella* is a coprophilous fungi and grows on musk-ox dung, and the presence of *Sporormiella* therefor suggests prescence of musk ox. Findings of musk-ox bones from Washington Land have been dated to ~3500 cal BP (Bennike, 2002), which is when a transition to cooler conditions was recorded in the sediments from Red-Throated Loon Lake, however it is also possible that the presence of musk-ox had an effect on the catchment vegetation and erosion that is recorded in the lake sediments. Since a reference genome is available for musk-ox, a new, highly resolved, palaeogenetic record from Washington Land could provide further insights into when Washington Land was colonized by musk-ox. Such a record could be compared with the geochemical and palaeoecological data presented in this thesis and thereby provide a better understanding of the environmental history of this part of northern Greenland.

5 Conclusions

This thesis presents the first well-dated sediment record from a lake in Washington Land in northern Greenland, as well as a framework of proxy records reflecting the environmental history of the lake and its surroundings. The following are the main conclusions of the study.

- Radiocarbon dates obtained on terrestrial plant remains from the base of the sequence yielded an age of about 7300 cal BP, thereby providing a minimum age of the local deglaciation.
- Pollen influx is generally very low and dominated by *Salix*, Cyperaceae, Poaceae and *Saxifraga*, which is consistent with the present vegetation of Washington Land.
- The sequence can be divided into two lithostratigraphic units; unit 1 is composed of clay and unit 2 of silty gyttja. The two units together represent three distinct stages of the environmental history.
- Unit 1 was deposited between 7300 and 5500 cal BP. Elemental geochemical analyses reveal relatively high influx of Si, K and Ca, which indicates high rates of catchment erosion and suggest that the lake was situated relatively close to the receding ice margin. This interpretation is supported by the abundance of *Salix*, which likely thrived on the newly exposed glacier forelands.
- The transition to gyttja, decrease in Si and K and increase in Ti, Fe and Rb, combined with a rapid increase in TOC content, as well as an increasing trend of Br, suggest that the environment in the catchment changed around 5500 cal BP. As the soils stabilised, physical erosion likely became less prevalent, and clearer lake water likely boosted the aquatic productivity. An increase in chemical weathering may explain the increasing trends of elements such as Ti, Fe and Rb. A substantial decrease in Ca and the complete absence of ostracods could reflect post-depositional dissolution of carbonates in the sediments. This period is interpreted as the Holocene Thermal Maximum of Washington Land, a period that previous studies describe as relatively warm and with elevated precipitation, consistent with increased chemical weathering and aquatic productivity, as well as with slightly elevated influx of unidentified spores and Cyperaceae pollen.
- Decreasing trends of most lithogenic elements and TOC content mark the end of the HTM and the onset of neoglacial cooling, consistent with previous studies. Several short-term trends can be recognized in most of the geochemical profiles and are likely related to climate fluctuations during the last 2000 years.

6 Acknowledgements

First and foremost, I would like to thank my main supervisor, Dan Hammarlund, for providing advice, support, and useful discussion throughout this project. I would also like to thank my co-supervisors, Anne Birgitte Nielsen and Karl Ljung, for helping me with the analyses. I am grateful for everyone at the Centre for Paleogenetics in Stockholm, who made this project possible in the first place, and provided insight along the way. Thank you, Malin Kylander at Stockholm University, for providing help and advice regarding the XRF analysis. Thank you, Renée Enevold at the Moesgaard Museum in Århus for aiding the identification of spores. Many thanks to Mats Rundgren, my examiner, for support with pollen identification and constructive comments on my work. Thank you, Robin Johansson, for assisting me with GIS and data handling. Lastly, thank you Kannika Wangritthikraikul for being my partner in crime, whom I can always rely on and laugh with.

7 References

Andresen, C. S., McCarthy, D. J., Valdemar Dylmer, C., Seidenkrantz, M.-S., Kuijpers, A., & Lloyd, J. M. (2011). Interaction between subsurface ocean waters and calving of the Jakobshavn Isbræ dur-ing the late Holocene. *The Holocene, 21*(2), 211–224. https://doi.org/10.1177/0959683610378877

ArtDatabanken (n.d.) Staggstarr. Artfakta. Retrieved 2023-04-06 from https://artfakta.se/artinformation/taxa/carex-nardina-264/detaljer

Axford, Y., Lasher, G. E., Kelly, M. A., Osterberg, E. C., Landis, J., Schellinger, G. C., Pfeiffer, A., Thompson, E., & Francis, D. R. (2019). Holocene temperature history of northwest Greenland – With new ice cap constraints and chironomid assemblages from Deltasø. *Quaternary Science Reviews, 215*, 160–172. https://doi.org/10.1016/j.quascirev.2019.05.011

Axford, Y., Losee, S., Briner, J. P., Francis, D. R., Langdon, P. G., & Walker, I. R. (2013). Holocene temperature history at the western Greenland Ice Sheet margin reconstructed from lake sediments. *Quaternary Science Reviews, 59*, 87–100. https://doi.org/10.1016/j.quascirev.2012.10.024

Balascio, N. L., D'Andrea, W. J., Bradley, R. S., & Perren, B. B. (2013). Biogeochemical evidence for hydrologic changes during the Holocene in a lake sediment record from southeast Greenland. *The Holocene, 23*(10), 1428–1439. https://doi.org/10.1177/0959683613493938

Bassett, I. J., Crompton, C. W., & Parmelee, J. A. (1978). *An atlas of airborne pollen grains and common fungus spores of Canada.* Dept. of Agriculture, Research Branch ; available from Print. and Pub. Supply and Services Canada.

Bennike, O. (2000). Palaeoecological studies of Holocene lake sediments from west Greenland. *Palaeogeography, Palaeoclimatology, Palaeoecology, 155*(3), 285–304. https://doi.org/10.1016/S0031-0182(99)00121-2

Bennike, O. (2002). Late Quaternary history of Washington Land, North Greenland. *Boreas, 31*(3), 260–272. https://doi.org/10.1111/j.1502-3885.2002.tb01072.x

Bennike, O., & Andreasen, C. (2005). New dates of musk-ox (Ovibos moschatus) remains from northwest Greenland. *Polar Record, 41*(2), 125–129. https://doi.org/10.1017/S0032247404004127

Bennike, O., Dawes, P. R., Funder, S., Kelly, M., & Weidick, A. (1987). The late Quaternary history of Hall Land, northwest Greenland: Discussion. *Canadian Journal of Earth Sciences, 24*(2), 370–374. https://doi.org/10.1139/e87-037

Berglund, B.E., Ralska-Jasiewiczowa, M., 1986. Pollen analysis and pollen diagrams, in: Berglund, B.E. (Ed.), *Handbook of Holocene Palaeoecology and Palaeohydrology*. Wiley, pp. 455-484.

Bergström, A., Jonsson, A., & Jansson, M. (2008). Phytoplankton responses to nitrogen and phos-phorus enrichment in unproductive Swedish lakes along a gradient of atmospheric nitrogen deposi-tion. *Aquatic Biology, 4*, 55–64. https://doi.org/10.3354/ab00099

Björck, S., Wohlfarth, B., Bennike, O., Hjort, C., & Persson, T. (1994). Revision of the early Holocene lake sediment based chronology and event stratigraphy on Hochstetter Forland, NE Greenland. *Boreas, 23*(4), 513–523. https://doi.org/10.1111/j.1502-3885.1994.tb00619.x

Blaauw, M. (2010). Methods and code for 'classical' age-modelling of radiocarbon sequences. *Quaternary Geochronology, 5*(5), 512–518. https://doi.org/10.1016/j.quageo.2010.01.002

Blake, W., Jr., Boucherle, M. M., Fredskild, B., Janssen, J. A., & Smol, J. P. (1992). The geomorphological setting, glacial history and Holocene development of 'Kap Inglefield Sø', Inglefield Land, North-West Greenland. *Meddelelser Om Grønland, 1992*(27), 1–42.

Boulanger-Lapointe, N., Lévesque, E., Boudreau, S., Henry, G. H. R., & Schmidt, N. M. (2014). Population structure and dynamics of Arctic willow (Salix arctica) in the High Arctic. *Journal of Biogeography, 41(*10), 1967–1978. https://doi.org/10.1111/jbi.12350

Briner, J. P., Michelutti, N., Francis, D. R., Miller, G. H., Axford, Y., Wooller, M. J., & Wolfe, A. P. (2006). A multi-proxy lacustrine record of Holocene climate change on northeastern Baffin Island, Arctic Canada. *Quaternary Research, 65*(3), 431–442. https://doi.org/10.1016/j.yqres.2005.10.005

Brodie, C. R., Leng, M. J., Casford, J. S. L., Kendrick, C. P., Lloyd, J. M., Yongqiang, Z., & Bird, M. I. (2011). Evidence for bias in C and N concentrations and δ13C composition of terrestrial and aquatic organic materials due to pre-analysis acid preparation methods. *Chemical Geology, 282*(3), 67–83. https://doi.org/10.1016/j.chemgeo.2011.01.007

Bunbury, J., & Gajewski, K. (2009). Biogeography of Freshwater Ostracodes in the Canadian Arctic Archipelago. *Arctic, 62*(3), 324–332.

Campos, P. F., Willerslev, E., Sher, A., Orlando, L., Axelsson, E., Tikhonov, A., Aaris-Sørensen, K., Greenwood, A. D., Kahlke, R.-D., Kosintsev, P., Krakhmalnaya, T., Kuznetsova, T., Lemey, P., MacPhee, R., Norris, C. A., Shepherd, K., Suchard, M. A., Zazula, G. D., Shapiro, B., & Gilbert, M. T. P. (2010). Ancient DNA analyses exclude humans as the driving force behind late Pleistocene musk ox (Ovibos moschatus) population dynamics. *Proceedings of the National Academy of Sciences, 107*(12), 5675–5680. https://doi.org/10.1073/pnas.0907189107

Cofaigh, C., Dowdeswell, J. A., Jennings, A. E., Hogan, K. A., Kilfeather, A., Hiemstra, J. F., Noormets, R., Evans, J., McCarthy, D. J., Andrews, J. T., Lloyd, J. M., & Moros, M. (2013). An extensive and dynamic ice sheet on the West Greenland shelf during the last glacial cycle. *Geology, 41*(2), 219–222. https://doi.org/10.1130/G33759.1

Cuven, S., Francus, P., & Lamoureux, S. (2011). Mid to Late Holocene hydroclimatic and geochemi-cal records from the varved sediments of East Lake, Cape Bounty, Canadian High Arctic. *Quaternary Science Reviews, 30*(19), 2651–2665. https://doi.org/10.1016/j.quascirev.2011.05.019

Cuven, S., Francus, P., & Lamoureux, S. F. (2010). Estimation of grain size variability with micro X-ray fluorescence in laminated lacustrine sediments, Cape Bounty, Canadian High Arctic. *Journal of Paleolimnology, 44*(3), 803–817. https://doi.org/10.1007/s10933-010-9453-1

Czymzik, M., Dulski, P., Plessen, B., von Grafenstein, U., Naumann, R., & Brauer, A. (2010). A 450 year record of spring-summer flood layers in annually laminated sediments from Lake Ammersee (southern Germany). *Water Resources Research, 46*(11). https://doi.org/10.1029/2009WR008360

Dahl-Jensen, D., Mosegaard, K., Gundestrup, N., Clow, G. D., Johnsen, S. J., Hansen, A. W., & Balling, N. (1998). Past Temperatures Directly from the Greenland Ice Sheet. *Science, 282*(5387), 268–271. https://doi.org/10.1126/science.282.5387.268

Dalton, A. S., Margold, M., Stokes, C. R., Tarasov, L., Dyke, A. S., Adams, R. S., Allard, S., Arends, H. E., Atkinson, N., Attig, J. W., Barnett, P. J., Barnett, R. L., Batterson, M., Bernatchez, P., Borns, H. W., Breckenridge, A., Briner, J. P., Brouard, E., Campbell, J. E., … Wright, H. E. (2020). An updated radiocarbon-based ice margin chronology for the last deglaciation of the North American Ice Sheet Complex. *Quaternary Science Reviews, 234*, 106223. https://doi.org/10.1016/j.quascirev.2020.106223

Davies, S. J., Lamb, H. F., & Roberts, S. J. (2015). Micro-XRF Core Scanning in Palaeolimnology: Recent Developments. In I. W. Croudace & R. G. Rothwell (Eds*.), Micro-XRF Studies of Sediment Cores: Applications of a non-destructive tool for the environmental sciences* (pp. 189–226). Springer Netherlands. https://doi.org/10.1007/978-94-017-9849-5_7

Dean, W. E. (1999). The carbon cycle and biogeochemical dynamics in lake sediments. *Journal of Paleolimnology, 21*, 375–393.

Dowdeswell, J. A., Hogan, K. A., Ó Cofaigh, C., Fugelli, E. M. G., Evans, J., & Noormets, R. (2014). Late Quaternary ice flow in a West Greenland fjord and cross-shelf trough system: Submarine land-forms from Rink Isbrae to Uummannaq shelf and slope. *Quaternary Science Reviews, 92.* 292–309. https://doi.org/10.1016/j.quascirev.2013.09.007

England, J. (1985). The late Quaternary history of Hall Land, northwest Greenland. *Canadian Journal of Earth Sciences, 22*(10), 1394–1408. https://doi.org/10.1139 /e85-147

England, J. (1999). Coalescent Greenland and Inuitian ice during the Last Glacial Maximum: Revising the Quaternary of the Canadian High Arctic. *Quaternary Science Reviews, 18*(3), 421–456. https://doi.org/10.1016/S0277-3791(98)00070-5

England, J., & Bradley, R. S. (1978). Past glacial activity in the Canadian high Arctic. *Science, 200*, 265–270.

Engstrom, D. R., Fritz, S. C., Almendinger, J. E., & Juggins, S. (2000). Chemical and biological trends during lake evolution in recently deglaciated terrain. *Nature, 408*(6809), https://doi.org/10 .1038/35041500

Epp, L. S., Gussarova, G., Boessenkool, S., Olsen, J., Haile, J., Schrøder-Nielsen, A., Ludikova, A., Hassel, K., Stenøien, H. K., Funder, S., Willerslev, E., Kjær, K., & Brochmann, C. (2015). Lake sedi-ment multitaxon DNA from North Greenland records early postglacial appearance of vascular plants and accurately tracks environmental changes. *Quaternary Science Reviews. 117.* 152–163. https://doi.org/10.1016/j.quascirev.2015.03.027

Evans, J., Ó Cofaigh, C., Dowdeswell, J. A., & Wadhams, P. (2009). Marine geophysical evidence for former expansion and flow of the Greenland Ice Sheet across the north-east Greenland continental shelf. *Journal of Quaternary Science. 24*(3), 279–293. https://doi.org/10.1002/jqs.1231

Faegri, K., Iversen, J., Kaland, P. E., & Krzywinski, K. (1989). *Textbook of pollen analysis* (4th ed.). Blackburn Press.

Farnsworth, L. B., Kelly, M. A., Bromley, G. R. M., Axford, Y., Osterberg, E. C., Howley, J. A., Jackson, M. S., & Zimmerman, S. R. (2018). Holocene history of the Greenland Ice-Sheet margin in Northern Nunatarssuaq, Northwest Greenland. *Arktos, 4*(1), 1–27. https://doi.org/10.1007/s41063-018-0044-0

Fedotov, A. P., Phedorin, M. A., Enushchenko, I. V., Vershinin, K. E., Melgunov, M. S., & Khodzher, T. V. (2012). A reconstruction of the thawing of the permafrost during the last 170years on the Tai-myr Peninsula (East Siberia, Russia). *Global and Planetary Change, 98–99*, 139–152. https://doi.org/10.1016/j.gloplacha.2012.09.002

Fredskild, B. (1973). Studies in the vegetational history of Greenland: paleopbotanical investigations of some Holocene lake and bog deposits. *Meddelelser om Grønland, 4.*

Fredskild, B. (1991). The genus Betula in Greenland-Holocene history, present distribution and synecology. *Nordic Journal of Botany, 11*(4), 393–412.

https://doi.org/10.1111/j.1756-1051.1991.tb01236.x

Fredskild, B. (1995). Palynology and sediment slumping in a high arctic Greenland lake. *Boreas, 24*(4), 345–354. https://doi.org/10.1111/j.1502-3885.1995.tb00784.x

Fuge, R. (1988). Sources of halogens in the environment, influences on human and animal health. *Environmental Geochemistry and Health, 10*(2), 51–61. https://doi.org/10.1007/BF01758592

Funder, S., & Abrahamsen, N. (1988). Palynology in a polar desert, eastern North Greenland. *Boreas, 17*(2), 195–207. https://doi.org/10.1111/j.1502-3885.1988.tb00546.x

Funder, S., Goosse, H., Jepsen, H., Kaas, E., Kjær, K. H., Korsgaard, N. J., Larsen, N. K., Linderson, H., Lyså, A., Möller, P., Olsen, J., & Willerslev, E. (2011). A 10,000-Year Record of Arctic Ocean Sea-Ice Variability—View from the Beach. *Science, 333*(6043), 747–750. https://doi.org/10.1126/science.1202760

Funder, S., & Hansen, L. (1996). The Greenland ice sheet—A model for its culmination anddecay during and after the last glacial maximum. *Bulletin of the Geological Society of Denmark, 42*, 137–152. https://doi.org/10.37570/bgsd-1995-42-12

Gajewski, K. (2015). Quantitative reconstruction of Holocene temperatures across the Canadian Arctic and Greenland. *Global and Planetary Change, 128*, 14–23. https://doi.org/10.1016/j.gloplacha.2015.02.003

Georgiadis, E., Giraudeau, J., Martinez, P., Lajeunesse, P., St-Onge, G., Schmidt, S., & Massé, G. (2018). Deglacial to postglacial history of Nares Strait, Northwest Greenland: A marine perspective from Kane Basin. *Climate of the Past, 14*(12), 1991–2010. https://doi.org/10.5194/cp-14-1991-2018

Giguet-Covex, C., Arnaud, F., Poulenard, J., Disnar, J.-R., Delhon, C., Francus, P., David, F., Enters, D., Rey, P.-J., & Delannoy, J.-J. (2011). Changes in erosion patterns during the Holocene in a cur-rently treeless subalpine catchment inferred from lake sediment geochemistry (Lake Anterne, 2063 m a.s.l., NW French Alps): The role of climate and human activities. *The Holocene, 21*(4), 651–665. https://doi.org/10.1177/0959683610391320

Haug, G. H., Hughen, K. A., Sigman, D. M., Peterson, L. C., & Röhl, U. (2001). Southward Migration of the Intertropical Convergence Zone Through the Holocene. *Science, 293*(5533), 1304–1308. https://doi.org/10.1126/science.1059725

Helama, S., Jones, P. D., & Briffa, K. R. (2017). Dark Ages Cold Period: A literature review and direc-tions for future research. *The Holocene, 27*(10), 1600–1606. https://doi.org/10.1177/0959683617693898

Hicks, S., & Hyvärinen, H. (1999). Pollen influx values measured in different sedimentary environ-ments and their palaeoecological implications. *Grana, 38*(4), 228–242. https://doi.org/10.1080/00173130075004618

Hill, E. A., Carr, J. R., & Stokes, C. R. (2017). A Review of Recent Changes in Major Marine-Terminating Outlet Glaciers in Northern Greenland. *Frontiers in Earth Science, 4*. https://www.frontiersin.org/articles/10.3389/feart.2016.00111

Hobbie, J. E., Shaver, G. R., Rastetter, E. B., Cherry, J. E., Goetz, S. J., Guay, K. C., Gould, W. A., & Kling, G. W. (2017). Ecosystem responses to climate change at a Low Arctic and a High Arctic long-term research site. *Ambio, 46*(1), 160–173. https://doi.org/10.1007/s13280-016-0870-x

Hobbs, W. O., Telford, R. J., Birks, H. J. B., Saros, J. E., Hazewinkel, R. R. O., Perren, B. B., Saulnier-Talbot, É., & Wolfe, A. P. (2010). Quantifying Recent Ecological Changes in Remote Lakes of North America and Greenland Using Sediment Diatom Assemblages. *PLOS ONE, 5*(4), e10026. https://doi.org/10.1371/journal.pone.0010026

Holmquist, J. R., Booth, R. K., & MacDonald, G. M. (2016). Boreal peatland water table depth and carbon accumulation during the Holocene thermal maximum, Roman Warm Period, and Medieval Climate Anomaly. *Palaeogeography, Palaeoclimatology, Palaeoecology, 444*, 15–27. https://doi.org/10.1016/j.palaeo.2015.11.035

Høye, T. T., Post, E., Meltofte, H., Schmidt, N. M., & Forchhammer, M. C. (2007). Rapid advance-ment of spring in the High Arctic. Current Biology, 17(12), R449–R451. https://doi.org/10.1016/j.cub.2007.04.047
Hughes, M., & Diaz, H. (1994). WAS THERE A 'MEDIEVAL WARM PERIOD', AND IF SO, WHERE AND WHEN? *Climatic Change, 26*, 109–142.

Hurst, J. M. (1980). Silurian stratigraphy and facies distribution in Washington Land and western Hall Land, North Greenland. *Bulletin Grønlands Geologiske Undersøgelse, 138*, 1–95. https://doi.org/10.34194/bullggu.v138.6680

Hyvärinen, H. (1985). Holocene pollen stratigraphy of Baird Inlet, east-central Ellesmere Island, arctic Canada. *Boreas, 14*(1), 19–32. https://doi.org/10.1111/j.1502-3885.1985.tb00884.x

Jakobsen, B. H., Fredskild, B., & Pedersen, J. B. T. (2008). Holocene changes in climate and vegeta-tion in the Ammassalik area, East Greenland, recorded in lake sediments and soil profiles. *Geografisk Tidsskrift-Danish Journal of Geography, 108*(1), 21–50. https://doi.org/10.1080/00167223.2008.10649573

Jakobsson, M., Hogan, K. A., Mayer, L. A., Mix, A., Jennings, A., Stoner, J., Eriksson, B., Jerram, K., Mohammad, R., Pearce, C., Reilly, B., & Stranne, C. (2018). The Holocene retreat dynamics and stability of

Petermann Glacier in northwest Greenland. *Nature Communications, 9(1)*, Article 1. https://doi.org/10.1038/s41467-018-04573-2

Jennings, A. E., Andrews, J. T., Oliver, B., Walczak, M., & Mix, A. (2019). Retreat of the Smith Sound Ice Stream in the Early Holocene. *Boreas, 48*(4), 825–840. https://doi.org/10.1111/bor.12391

Jensen, D., & Cappelen, J. (2021). Climatological Standard Normals 1991-2020—Greenland.

Jomelli, V., Lane, T., Favier, V., Masson-Delmotte, V., Swingedouw, D., Rinterknecht, V., Schimmelpfennig, I., Brunstein, D., Verfaillie, D., Adamson, K., Leanni, L., Mokadem, F., Aumaître, G., Bourlès, D. L., & Keddadouche, K. (2016). Paradoxical cold conditions during the medieval climate anomaly in the Western Arctic. *Scientific Reports, 6*(1), https://doi.org/10.1038/srep32984

Kalugin, I., Darin, A., Rogozin, D., & Tretyakov, G. (2013). Seasonal and centennial cycles of car-bonate mineralisation during the past 2500 years from varved sediment in Lake Shira, South Sibe-ria. *Quaternary International, 290–291*, 245–252. https://doi.org/10.1016/j.quaint.2012.09.016

Kaplan, M. R., Wolfe, A. P., & Miller, G. H. (2002). Holocene Environmental Variability in Southern Greenland Inferred from Lake Sediments. *Quaternary Research, 58*(2), 149–159. https://doi.org/10.1006/qres. 2002.2352

Kaufman, D. S., Ager, T. A., Anderson, N. J., Anderson, P. M., Andrews, J. T., Bartlein, P. J., Bru-baker, L. B., Coats, L. L., Cwynar, L. C., Duvall, M. L., Dyke, A. S., Edwards, M. E., Eisner, W. R., Gajewski, K., Geirsdóttir, A., Hu, F. S., Jennings, A. E., Kaplan, M. R., Kerwin, M. W., … Wolfe, B. B. (2004). Holocene thermal maximum in the western Arctic (0–180°W). *Quaternary Science Reviews, 23*(5), 529–560. https://doi.org/10.1016/j.quascirev.2003.09.007

Kelly, M., & Bennike, O. (1992). Quaternary geology of western and central North Greenland. *Rapport Grønlands Geologiske Undersøgelse, 153*, 1–34. https://doi.org/10.34194/rapggu.v153.8164

Kjær, K. H., Bjørk, A. A., Kjeldsen, K. K., Hansen, E. S., Andresen, C. S., Siggaard-Andersen, M.-L., Khan, S. A., Søndergaard, A. S., Colgan, W., Schomacker, A., Woodroffe, S., Funder, S., Rouillard, A., Jensen, J. F., & Larsen, N. K. (2022). Glacier response to the Little Ice Age during the Neoglacial cooling in Greenland. *Earth-Science Reviews, 227*, 103984. https://doi.org/10.1016/j.earscirev.2022.103984

Klein, D. R., Bruun, H. H., Lundgren, R., & Philipp, M. (2008). Climate Change Influences on Species Interrelationships and Distributions in High-Arctic Greenland. In *Advances in Ecological Research* (Vol. 40, pp. 81–100). Academic Press. https://doi.org/10.1016/S0065-2504(07)00004-9

Koinig, K. A., Shotyk, W., Lotter, A. F., Ohlendorf, C., & Sturm, M. (2003). 9000 years of geochemical evolution of lithogenic major and trace elements in the sediment of an alpine lake – the role of climate, vegetation, and land- use history. *Journal of Paleolimnology, 30.* 307-320.

Komuro, Y., & Hasumi, H. (2005). Intensification of the Atlantic Deep Circulation by the Canadian Archipelago Throughflow. *Journal of Physical Oceanography, 35*(5), 775–789. https://doi.org/10.1175/JPO2709.1

Krawczyk, D., Witkowski, A., Moros, M., Lloyd, J., Kuijpers, A., & Kierzek, A. (2010). Late-Holocene diatom-inferred reconstruction of temperature variations of the West Greenland Current from Disko Bugt, central West Greenland. *The Holocene, 20*(5), 659–666. https://doi.org/10.1177/0959683610371993

Kusch, S., Bennike, O., Wagner, B., Lenz, M., Steffen, I., & Rethemeyer, J. (2019). Holocene envi-ronmental history in high-Arctic North Greenland revealed by a combined biomarker and macrofossil approach. *Boreas, 48*(2), 273–286. https://doi.org/10.1111/bor.12377

Kylander, M. E., Ampel, L., Wohlfarth, B., & Veres, D. (2011). High-resolution X-ray fluorescence core scanning analysis of Les Echets (France) sedimentary sequence: New insights from chemical proxies. *Journal of Quaternary Science, 26*(1), 109–117. https://doi.org/10.1002/jqs.1438

Lamb, H. H. (1965). The early medieval warm epoch and its sequel. *Palaeogeography, Palaeoclimatology, Palaeoecology, 1.* 13–37. https://doi.org/10.1016/0031-0182(65)90004-0

Landvik, J., Weidick, A., & Hansen, A. (2001). The glacial history of the Hans Tausen Iskappe and the last glaciation of Peary Land, North Greenland. *Meddelelser Om Grønland, Geoscience, 39,* 27–44.

Larsen, N. K., Kjær, K. H., Funder, S., Möller, P., van der Meer, J. J. M., Schomacker, A., Linge, H., & Darby, D. A. (2010). Late Quaternary glaciation history of northernmost Greenland – Evidence of shelf-based ice. *Quaternary Science Reviews, 29*(25), 3399–3414. https://doi.org/10.1016/j.quascirev.2010.07.027

Lecavalier, B. S., Milne, G. A., Simpson, M. J. R., Wake, L., Huybrechts, P., Tarasov, L., Kjeldsen, K. K., Funder, S., Long, A. J., Woodroffe, S., Dyke, A. S., & Larsen, N. K. (2014). A model of Greenland ice sheet deglaciation constrained by observations of relative sea level and ice extent. *Quaternary Science Reviews, 102*, 54–84. https://doi.org/10.1016/j.quascirev.2014.07.018

Ljungqvist, F. C. (2010). A New Reconstruction of Temperature Variability in the Extra-Tropical Northern Hemisphere During the Last Two Millennia. *Geografiska Annaler: Series A, Physical Geog-raphy, 92*(3), 339–351. https://doi.org/10.1111/j.1468-

0459.2010.00399.x

McFarlin, J. M., Axford, Y., Osburn, M. R., Kelly, M. A., Osterberg, E. C., & Farnsworth, L. B. (2018). Pronounced summer warming in northwest Greenland during the Holocene and Last Interglacial. *Proceedings of the National Academy of Sciences, 115*(25), 6357–6362. https://doi.org/10.1073/pnas.1720420115

McGeehan, T., & Maslowski, W. (2012). Evaluation and control mechanisms of volume and fresh-water export through the Canadian Arctic Archipelago in a high-resolution pan-Arctic ice-ocean model. *Journal of Geophysical Research: Oceans, 117*(C8). https://doi.org/10.1029/2011JC007261

Meyers, P. A. (2003). Applications of organic geochemistry to paleolimnological reconstructions: A summary of examples from the Laurentian Great Lakes. *Organic Geochemistry, 34*(2), 261–289. https://doi.org/10.1016/S0146-6380(02)00168-7

Miettinen, A., Divine, D. V., Husum, K., Koç, N., & Jennings, A. (2015). Exceptional ocean surface conditions on the SE Greenland shelf during the Medieval Climate Anomaly. *Paleoceanography, 30*(12), 1657–1674. https://doi.org/10.1002/2015PA002849

Möller, P., Larsen, N. K., Kjær, K. H., Funder, S., Schomacker, A., Linge, H., & Fabel, D. (2010). Early to middle Holocene valley glaciations on northernmost Greenland. *Quaternary Science Reviews, 29*(25), 3379–3398. https://doi.org/10.1016/j.quascirev.2010.06.044

Moros, M., Jansen, E., Oppo, D. W., Giraudeau, J., & Kuijpers, A. (2012). Reconstruction of the late-Holocene changes in the Sub-Arctic Front position at the Reykjanes Ridge, north Atlantic. *The Holocene, 22*(8), 877–886. https://doi.org/10.1177/0959683611434224

Mouginot, J., Rignot, E., Bjørk, A. A., van den Broeke, M., Millan, R., Morlighem, M., Noël, B., Scheuchl, B., & Wood, M. (2019). Forty-six years of Greenland Ice Sheet mass balance from 1972 to 2018. *Proceedings of the National Academy of Sciences, 116*(19), 9239–9244. https://doi.org/10.1073/pnas.1904242116

O'Brien, S. R., Mayewski, P. A., Meeker, L. D., Meese, D. A., Twickler, M. S., & Whitlow, S. I. (1995). Complexity of Holocene Climate as Reconstructed from a Greenland Ice Core. *Science, 270*(5244), 1962–1964.

Oldfield, F., Wake, R., Boyle, J., Jones, R., Nolan, S., Gibbs, Z., Appleby, P., Fisher, E., & Wolff, G. (2003). The late-Holocene history of Gormire Lake (NE England) and its catchment: A multiproxy reconstruction of past human impact. *The Holocene, 13*(5), 677–690. https://doi.org/10.1191/0959683 603hl654rp

Olsen, J., Anderson, N. J., & Leng, M. J. (2013). Limnological controls on stable isotope records of late-Holocene palaeoenvironment change in SW Greenland: A paired lake study. *Quaternary Science Reviews, 66*, 85–95. https://doi.org/10.1016/j.quascirev.2012.10.043

Olsen, J., Kjær, K. H., Funder, S., Larsen, N. K., & Ludikova, A. (2012). High-Arctic climate conditions for the last 7000 years inferred from multi-proxy analysis of the Bliss Lake record, North Greenland. *Journal of Quaternary Science, 27*(3), 318–327. https://doi.org/10.1002/jqs.1548

Pedersen, M. W., Ginolhac, A., Orlando, L., Olsen, J., Andersen, K., Holm, J., Funder, S., Willerslev, E., & Kjær, K. H. (2013). A comparative study of ancient environmental DNA to pollen and macrofossils from lake sediments reveals taxonomic overlap and additional plant taxa. *Quaternary Science Reviews, 75*, 161–168. https://doi.org/10.1016/j.quascirev.2013.06.006

Peterson, L. C., Haug, G. H., Hughen, K. A., & Röhl, U. (2000). Rapid Changes in the Hydrologic Cycle of the Tropical Atlantic During the Last Glacial. *Science, 290*(5498), 1947–1951. https://doi.org/10.1126/science.290.5498.1947

Phedorin, M. A., Goldberg, E. L., Grachev, M. A., Levina, O. L., Khlystov, O. M., & Dolbnya, I. P. (2000). The comparison of biogenic silica, Br and Nd distributions in the sediments of Lake Baikal as proxies of changing paleoclimates of the last 480kyr. *Nuclear Instruments and Methods in Physics Research Section A: Accelerators, Spectrometers, Detectors and Associated Equipment, 448*(1), 400–406. https://doi.org/10.1016/S0168-9002(99)00726-3

Philippsen, B. (2013). The freshwater reservoir effect in radiocarbon dating. *Heritage Science, 1*(1), 24. https://doi.org/10.1186/2050-7445-1-24

Porsbjerg, C., Rasmussen, A., & Backer, V. (2003). Airborne pollen in Nuuk, Greenland, and the importance of meteorological parameters. *Aerobiologia, 19*. 29-37.

Presthus Heggen, M., Birks, H. H., & Anderson, N. J. (2010). Long-term ecosystem dynamics of a small lake and its catchment in west Greenland. *The Holocene, 20*(8), 1207–1222. https://doi.org/10.1177/0959683610371995

R Core Team (2011) R: a language and environment for statistical computing. R Foundation for Statistical Computing, Vienna, Austria.

Reilly, B. T., Stoner, J. S., Mix, A. C., Walczak, M. H., Jennings, A., Jakobsson, M., Dyke, L., Glueder, A., Nicholls, K., Hogan, K. A., Mayer, L. A., Hatfield, R. G., Albert, S., Marcott, S., Fallon, S., & Chese-by, M. (2019). Holocene break-up and reestablishment of the Petermann Ice Tongue, Northwest Greenland. *Quaternary Science Reviews, 218*, 322–342. https://doi.org/10.1016/j.quascirev.2019.06.023

Reimer, P. J., Austin, W. E. N., Bard, E., Bayliss, A., Blackwell, P. G., Ramsey, C. B., Butzin, M., Cheng, H., Edwards, R. L., Friedrich, M., Grootes, P. M., Guilderson, T. P., Hajdas, I., Heaton, T. J., Hogg, A. G., Hughen, K. A., Kromer, B., Manning, S. W., Muscheler, R., … Talamo, S. (2020). The IntCal20 Northern Hemisphere Radiocarbon Age Calibration Curve (0–55 cal kBP). *Radiocarbon, 62*(4), 725–757. https://doi.org/10.1017/RDC.2020.41

Ribeiro, S., Moros, M., Ellegaard, M., & Kuijpers, A. (2012). Climate variability in West Greenland during the past 1500 years: Evidence from a high-resolution marine palynological record from Disko Bay. *Boreas, 41*(1), 68–83. https://doi.org/10.1111/j.1502-3885.2011.00216.x

Rignot, E., & Kanagaratnam, P. (2006). Changes in the Velocity Structure of the Greenland Ice Sheet. *Science, 311*(5763), 986–990. https://doi.org/10.1126/science.1121381

Rousseau, D.-D., Schevin, P., Ferrier, J., Jolly, D., Andreasen, T., Ascanius, S. E., Hendriksen, S.-E., & Poulsen, U. (2008). Long-distance pollen transport from North America to Greenland in spring. *Journal of Geophysical Research: Biogeosciences, 113*(G2). https://doi.org/10.1029/2007JG000456

Schmidt, N. M., Baittinger, C., & Forchhammer, M. C. (2006). Reconstructing Century-long Snow Regimes Using Estimates of High Arctic Salix arctica Radial Growth. *Arctic, Antarctic, and Alpine Research, 38*(2), 257–262. https://doi.org/10.1657/1523-0430(2006)38

Shala, S., Helmens, K. F., Jansson, K. N., Kylander, M. E., Risberg, J., & Löwemark, L. (2014). Palaeoenvironmental record of glacial lake evolution during the early Holocene at Sokli, NE Finland. Boreas, 43(2), 362–376. https://doi.org/10.1111/bor.12043

Simpson, M. J. R., Milne, G. A., Huybrechts, P., & Long, A. J. (2009). Calibrating a glaciological model of the Greenland ice sheet from the Last Glacial Maximum to present-day using field observations of relative sea level and ice extent. *Quaternary Science Reviews, 28*(17), 1631–1657. https://doi.org/10.1016/j.quascirev.2009.03.004

Søndergaard, A. S., Larsen, N. K., Olsen, J., Strunk, A., & Woodroffe, S. (2019). Glacial history of the Greenland Ice Sheet and a local ice cap in Qaanaaq, northwest Greenland. *Journal of Quaternary Science, 34*(7), 536–547. https://doi.org/10.1002/jqs.3139

Stockmarr, J., 1971. Tablets with spores used in absolute pollen analysis. *Pollen et Spores 13*, 615-621.

Striberger, J., Björck, S., Holmgren, S., & Hamerlík, L. (2012). The sediments of Lake Lögurinn – A unique proxy record of Holocene glacial meltwater variability in eastern Iceland. *Quaternary Science Reviews, 38*, 76–88. https://doi.org/10.1016/j.quascirev.2012.02.001

Talbot, M. R., & Lærdal, T. (2000). The Late Pleistocene—Holocene palaeolimnology of Lake Victoria, East Africa, based upon elemental and isotopic analyses of sedimentary organic matter. Journal of Paleolimnology, 23(2), 141–164. https://doi.org/10.1023/A:1008029400463

Vinther, B. M., Buchardt, S. L., Clausen, H. B., Dahl-Jensen, D., Johnsen, S. J., Fisher, D. A., Koerner, R. M., Raynaud, D., Lipenkov, V., Andersen, K. K., Blunier, T., Rasmussen, S. O., Steffensen, J. P., & Svensson, A. M. (2009). Holocene thinning of the Greenland ice sheet. *Nature, 461*(7262), Article 7262. https://doi.org/10.1038/nature08355

Wagner, B., & Bennike, O. (2015). Holocene environmental change in the Skallingen area, eastern North Greenland, based on a lacustrine record. *Boreas, 44*(1), 45–59. https://doi.org/10.1111/bor.12085

Wagner, B., Melles, M., Hahne, J., Niessen, F., & Hubberten, H.-W. (2000). Holocene climate history of Geographical Society Ø, East Greenland—Evidence from lake sediments. *Palaeogeography, Palaeoclimatology, Palaeoecology, 160*(1), 45–68. https://doi.org/10.1016/S0031-0182(00)00046-8

Weltje, G., Bloemsma, M., Tjallingii, R., Heslop, D., Röhl, U., Croudace, I., & Croudace, I. (2015). Prediction of Geochemical Composition from XRF Core Scanner Data: A New Multivariate Approach Including Automatic Selection of Calibration Samples and Quantification of Uncertainties (pp. 507–534). https://doi.org/10.1007/978-94-017-9849-5_21

Winkelmann, D., Jokat, W., Jensen, L., & Schenke, H.-W. (2010). Submarine end moraines on the continental shelf off NE Greenland – Implications for Lateglacial dynamics. *Quaternary Science Reviews, 29*(9), 1069–1077. https://doi.org/10.1016/j.quascirev.2010.02.002

Yarincik, K. M., Murray, R. W., & Peterson, L. C. (2000). Climatically sensitive eolian and hemipelagic deposition in the Cariaco Basin, Venezuela, over the past 578,000 years: Results from Al/Ti and K/Al. *Paleoceanography, 15*(2), 210–228. https://doi.org/10.1029/1999PA900048

Young, N. E., Schweinsberg, A. D., Briner, J. P., & Schaefer, J. M. (2015). Glacier maxima in Baffin Bay during the Medieval Warm Period coeval with Norse settlement. *Science Advances, 1*(11), e1500806. https://doi.org/10.1126/sciadv.1500806

Zreda, M., England, J., Phillips, F., Elmore, D., & Sharma, P. (1999). Unblocking of the Nares Strait by Greenland and Ellesmere ice-sheet retreat 10,000 years ago. *Nature, 398*(6723), Article 6723. https://doi.org/10.1038/18197

Appendix A

Correlation matrices.

Correlation matrix of the CLR-transformed XRF data.

	Si	*S*	*K*	*Ca*	*Ti*	*Mn*	*Fe*	*Br*	*Rb*	*Sr*
Si	1									
S	-0,84066	1								
K	0,867125	-0,86937	1							
Ca	0,560801	-0,39562	0,241443	1						
Ti	-0,20152	-0,01238	0,196203	-0,89107	1					
Mn	0,911512	-0,88477	0,942393	0,423518	-0,01332	1				
Fe	-0,39621	0,23238	0,008126	-0,88461	0,903855	-0,19276	1			
Br	-0,95954	0,812968	-0,89107	-0,61214	0,233328	-0,94007	0,366825	1		
Rb	-0,46427	0,162226	-0,10738	-0,91224	0,875591	-0,29268	0,812412	0,496026	1	
Sr	-0,22249	0,379623	-0,55678	0,626737	-0,87508	-0,38307	-0,72183	0,165861	-0,68557	1

Correlation matrix of the CLR-transformed XRF data, unit 1.

	Si	*S*	*K*	*Ca*	*Ti*	*Mn*	*Fe*	*Br*	*Rb*	*Sr*
Si	1									
S	-0,6072	1								
K	0,80677	-0,77468	1							
Ca	0,784892	-0,29292	0,526374	1						
Ti	-0,2739	-0,30997	0,133773	-0,69248	1					
Mn	0,704581	-0,69901	0,673567	0,490184	0,004068	1				
Fe	-0,53896	0,142801	-0,30818	-0,77242	0,649228	-0,33182	1			
Br	-0,81541	0,250398	-0,59347	-0,83261	0,447996	-0,61575	0,5183	1		
Rb	-0,22124	-0,29025	0,065386	-0,6516	0,750885	0,007884	0,549172	0,385209	1	
Sr	0,090863	0,144263	-0,17053	0,587105	-0,75725	-0,00593	-0,61377	-0,31897	-0,76409	1

Correlation matrix of the CLR-transformed XRF data, unit 2.

	Si	*S*	*K*	*Ca*	*Ti*	*Mn*	*Fe*	*Br*	*Rb*	*Sr*
Si	1									
S	-0,33719	1								
K	0,244853	-0,51021	1							
Ca	-0,34776	0,407517	-0,87947	1						
Ti	0,219125	-0,47801	0,960311	-0,92913	1					
Mn	0,142115	-0,39429	0,605204	-0,56182	0,587132	1				
Fe	0,012155	-0,21041	0,811386	-0,80521	0,843992	0,429053	1			
Br	-0,5871	0,216491	-0,60698	0,606326	-0,5749	-0,48428	-0,45914	1		
Rb	0,08015	-0,49168	0,510206	-0,67918	0,568797	0,224104	0,422034	-0,38536	1	
Sr	-0,42129	0,475172	-0,86932	0,962354	-0,90195	-0,60264	-0,75122	0,622441	-0,67694	1

Appendix B

Modelled age, depth and amount of pollen and spores in the analysed pollen samples.

SAMPLE NR.	1	3	5	7	10	14	18	22	26	30	34	38	41	44
AGE	395	539	689	843	1073	1375	1680	1995	2320	2651	2984	3315	3559	3801
DEPTH	15	19	23	27	33	41	49	57	65	73	81	89	95	101
LYCOPODIUM	2132	1532	1424	2204	1224	2311	1958	1592	1552	1522	1331	1620	1879	1544
UNIDENTIFIED SPORES	9040	5056	2763	6458	8776	5662	6461	3248	2111	4362	3338	16810	5283	4592
SALIX	1	5	2	5	2	5	3	2	2	3	1	5	2	2
CYPERACEAE	2	0	2	1	1	0	4	2	0	4	3	2	5	3
POACEAE	1	1	0	1	0	0	0	0	1	1	0	1	1	0
SAXIFRAGA	0	0	0	2	2	3	0	0	2	0	0	0	1	0
POLYPODIACEAE	0	0	0	0	0	0	0	0	9	0	1	0	0	0
CARYOPHYL-LACEAE	0	0	0	0	0	1	0	0	0	0	0	0	0	0
BRASSICACEAE	0	0	0	0	0	1	0	0	1	0	0	0	0	0
SPHAGNUM	0	0	0	0	0	1	1	0	1	0	0	0	0	0
BETULA	0	0	0	0	0	0	0	0	0	0	0	0	0	0
PINUS	0	0	0	0	0	0	0	0	0	0	1	0	0	1
ALNUS	0	0	0	0	0	0	0	0	0	0	0	0	0	1
ULMUS	0	1	0	0	0	0	0	0	0	0	0	0	0	0
UNIDENTIFIED	0	0	0	0	0	0	1	1	0	0	0	0	0	0

SAMPLE NR.	47	50	53	56	59	62	65	67	69	71	73	75	77	79
AGE	4049	4312	4601	4928	5298	5698	6103	6473	6787	7035	7210	1317	7390	7430
DEPTH	107	113	119	125	131	137	143	149	155	161	167	173	179	185
LYCOPODIUM	1741	1504	1497	1639	1566	1209	625	1190	1249	1563	1026	1004	1254	1688
UNIDENTIFIED SPORES	9968	14550	12393	19338	14274	5435	2061	3706	9710	3532	1262	1086	1957	842
SALIX	3	3	1	5	4	11	4	9	22	29	19	13	44	10
CYPERACEAE	4	1	1	2	6	7	0	1	2	2	0	0	1	0
POACEAE	0	0	0	0	0	1	0	0	0	2	0	0	1	0
SAXIFRAGA	0	1	0	2	2	0	1	0	0	0	0	0	0	0
POLYPODIACEAE	0	1	0	0	0	0	0	0	0	0	1	0	0	1
CARYOPHYL-LACEAE	0	0	0	0	0	0	0	0	0	0	0	0	0	0
BRASSICACEAE	0	0	0	0	0	0	2	0	0	0	0	1	0	0
SPHAGNUM	0	0	0	0	0	0	0	0	0	0	0	0	0	0
BETULA	0	0	0	0	0	0	0	0	1	0	0	0	0	0
PINUS	0	0	0	0	0	0	0	1	0	0	0	1	0	0
ALNUS	0	0	0	0	0	1	0	0	0	0	0	0	0	0
ULMUS	0	0	0	0	0	0	0	0	0	0	0	0	0	0
UNIDENTIFIED	0	0	0	0	0	0	0	0	0	2	0	1	0	1

Tidigare skrifter i serien ”Examensarbeten i Geologi vid Lunds universitet”:

608. Damber, Maja, 2020: A palaeoecological study of the establishment of beech forest in Söderåsen National Park, southern Sweden. (45 hp)
609. Karastergios, Stylianos, 2020: Characterization of mineral parageneses and metamorphic textures in eclogite- to high-pressure granulite-facies marble at Allmenningen, Roan, western Norway. (45 hp)
610. Lindberg Skutsjö, Love, 2021: Geologiska och hydrogeologiska tolkningar av SkyTEM-data från Vombsänkan, Sjöbo kommun, Skåne. (15 hp)
611. Hertzman, Hanna, 2021: Odensjön - A new varved lake sediment record from southern Sweden. (45 hp)
612. Molin, Emmy, 2021: Rare terrestrial vertebrate remains from the Pliensbachian (Lower Jurassic) Hasle Formation on the Island of Bornholm, Denmark. (45 hp)
613. Höjbert, Karl, 2021: Dendrokronologi - en nyckelmetod för att förstå klimat- och miljöförändringar i Jämtland under holocen. (15 hp)
614. Lundgren Sassner, Lykke, 2021: A Method for Evaluating and Mapping Terrestrial Deposition and Preservation Potential-for Palaeostorm Surge Traces. Remote Mapping of the Coast of Scania, Blekinge and Halland, in Southern Sweden, with a Field Study at Dalköpinge Ängar, Trelleborg. (45 hp)
615. Granbom, Johanna, 2021: En detaljerad undersökning av den mellanordoviciska ”furudalkalkstenen” i Dalarna. (15 hp)
616. Greiff, Johannes, 2021: Oolites from the Arabian platform: Archives for the aftermath of the end-Triassic mass extinction. (45 hp)
617. Ekström, Christian, 2021: Rödfärgade utfällningar i dammanläggningar orsakade av *G. ferruginea* och *L. ochracea* - Problemstatistik och mikrobiella levnadsförutsättningar. (15 hp)
618. Östsjö, Martina, 2021: Geologins betydelse i samhället och ett första steg mot en geopark på Gotland. (15 hp)
619. Westberg, Märta, 2021: The preservation of cells in biomineralized vertebrate tissues of Mesozoic age – examples from a Cretaceous mosasaur (Reptilia, Mosasauridae). (45 hp)
620. Gleisner, Lovisa, 2021: En detaljerad undersökning av kalkstenslager i den mellanordoviciska gullhögenformationen på Billingen i Västergötland. (15 hp)
621. Bonnevier Wallstedt, Ida, 2021: Origin and early evolution of isopods - exploring morphology, ecology and systematics. (15 hp)
622. Selezeneva, Natalia, 2021: Indications for solar storms during the Last Glacial Maximum in the NGRIP ice core. (45 hp)
623. Bakker, Aron, 2021: Geological characterisation of geophysical lineaments as part of the expanded site descriptive model around the planned repository site for high-level nuclear waste, Forsmark, Sweden. (45 hp)
624. Sundberg, Oskar, 2021: Jordlagerföljden i Höjeådalen utifrån nya borrningar. (15 hp)
625. Sartell, Anna, 2021: The igneous complex of Ekmanfjorden, Svalbard: an integrated field, petrological and geochemical study. (45 hp)
626. Juliusson, Oscar, 2021: Implications of ice -bedrock dynamics at Ullstorp, Scania, southern Sweden. (45 hp)
627. Eng, Simon, 2021: Rödslam i svenska kraftdammar - Problematik och potentiella lösningar. (15 hp)
628. Kervall, Hanna, 2021: Feasibility of Enhanced Geothermal Systems in the Precambrian crystalline basement in SW Scania, Sweden. (45 hp)
629. Smith, Thomas, 2022: Assessing the relationship between hypoxia and life on Earth, and implications for the search for habitable exoplanets. (45 hp)
630. Neumann, Daniel, 2022: En mosasaurie (Reptilia, Mosasauridae) av paleocensk ålder? (15 hp)
631. Svensson, David, 2022: Geofysisk och geologisk tolkning av kritskollors utbredning i Ystadsområdet. (15 hp)
632. Allison, Edward, 2022: Avsättning av Black Carbon i sediment från Odensjön, södra Sverige. (15 hp)
633. Jirdén, Elin, 2022: OSL dating of the Mesolithic site Nilsvikdalen 7, Bjorøy, Norway. (45 hp)
634. Wong, Danny, 2022: GIS-analys av effekten vid stormflod/havsnivåhöjning, Morupstrakten, Halland. (15 hp)
635. Lycke, Björn, 2022: Mikroplast i vattenavsatta sediment. (15 hp)
636. Schönherr, Lara, 2022: Grön fältspat i Varbergskomplexet. (15 hp)
637. Funck, Pontus, 2022: Granens ankomst och etablering i Skandinavien under postglacial tid. (15 hp)
638. Brotzen, Olga M., 2022: Geologiska besöksmål och geoparker som plattform för popularisering av geovetenskap. (15 hp)
639. Lodi, Giulia, 2022: A study of carbon, nitrogen, and biogenic silica concentra-

tions in *Cyperus papyrus*, the sedge dominating the permanent swamp of the Okavango Delta, Botswana, Africa. (45 hp)

640. Nilsson, Sebastian, 2022: PFAS- En sammanfattning av ny forskning, med ett fokus på föroreningskällor, provtagning, analysmetoder och saneringsmetoder. (15 hp)
641. Jägfeldt, Hans, 2022: Molnens påverkan på jordens strålningsbalans och klimatsystem. (15 hp)
642. Sundberg, Melissa, 2022: Paleontologiska egenskaper och syreisotopsutveckling i borrkärnan Limhamn-2018: Kopplingar till klimatförändringar under yngre krita. (15 hp)
643. Bjermo, Tim, 2022: A re-investigation of hummocky moraine formed from ice sheet decay using geomorphological and sedimentological evidence in the Vomb area, southern Sweden. (45 hp)
644. Halvarsson, Ellinor, 2022: Structural investigation of ductile deformations across the Frontal Wedge south of Lake Vättern, southern Sweden. (45 hp)
645. Brakebusch, Linus, 2022: Record of the end-Triassic mass extinction in shallow marine carbonates: the Lorüns section (Austria). (45 hp)
646. Wahlquist, Per, 2023: Stratigraphy and palaeoenvironment of the early Jurassic volcaniclastic strata at Djupadalsmölla, central Skåne, Sweden. (45 hp)
647. Gebremedhin, G. Gebreselassie, 2023: U-Pb geochronology of brittle deformation using LA-ICP-MS imaging on calcite veins. (45 hp)
648. Mroczek, Robert, 2023: Petrography of impactites from the Dellen impact structure, Sweden. (45 hp)
649. Gunnarsson, Niklas, 2023: Upper Ordovician stratigraphy of the Stora Sutarve core (Gotland, Sweden) and an assessment of the Hirnantian Isotope Carbon Excursion (HICE) in high-resolution. (45 hp)
650. Cordes, Beatrix, 2023: Vilken ny kunskap ger aDNA-analyser om vegetationsutvecklingen i Nordeuropa under och efter Weichsel-istiden? (15 hp)
651. Bonnevier Wallstedt, Ida, 2023: Palaeocolour, skin anatomy and taphonomy of a soft-tissue ichthyosaur (Reptilia, Ichthyopterygia) from the Toarcian (Lower Jurassic) of Luxembourg. (45 hp)
652. Kryffin, Isidora, 2023: Exceptionally preserved fish eyes from the Eocene Fur Formation of Denmark – implications for palaeobiology, palaeoecology and taphonomy. (45 hp)
653. Andersson, Jacob, 2023: Nedslagskratrars inverkan på Mars yt-datering. En undersökning av Mars främsta yt-dateringsmetod ”Crater Counting". (15 hp)
654. Sundberg, Melissa, 2023: A study in ink – the morphology, taphonomy and phylogeny of squid-like cephalopods from the Jurassic Posidonia Shale of Germany and the first record of a loligosepiid gill. (45 hp)
655. Häggblom, Joanna, 2023: En patologisk sjölilja från silur på Gotland, Sverige. (15 hp)
656. Bergström, Tim, 2023: Hur gammal är jordens inre kärna? (15 hp)
657. Bollmark, Viveka, 2023: Ca isotope, oceanic anoxic events and the calcareous nannoplankton. (15 hp)
658. Madsen, Ariella, 2023: Polycykliska aromatiska kolväten i Hanöbuktens kustnära sediment - En sedimentologisk undersökning av vikar i närhet av pappersbruk. (15 hp)
659. Wangritthikraikul, Kannika, 2023: Holocene Environmental History of Warming Land, Northern Greenland: a study based on lake sediments. (45 hp)
660. Kurop, Anna, 2023: Reconstruction of the glacier dynamics and Holocene chronology of retreat of Helagsglaciären in Central Sweden. (45 hp)
661. Frisendahl, Kajsa, 2023: Holocene environmental history of Washington Land, NW Greenland: a study based on lake sediments. (45 hp)

LUNDS UNIVERSITET

Geologiska institutionen
Lunds universitet
Sölvegatan 12, 223 62 Lund